



Citation for published version:

Arnott, R, Cherif, M, Bryant, L & Wain, D 2021, 'Artificially generated turbulence: A review of phycological nanocosm, microcosm, and mesocosm experiments', *Hydrobiologia*, vol. 848, pp. 961-991.
<https://doi.org/10.1007/s10750-020-04487-5>

DOI:

[10.1007/s10750-020-04487-5](https://doi.org/10.1007/s10750-020-04487-5)

Publication date:

2021

Document Version

Peer reviewed version

[Link to publication](#)

University of Bath

Alternative formats

If you require this document in an alternative format, please contact:
openaccess@bath.ac.uk

General rights

Copyright and moral rights for the publications made accessible in the public portal are retained by the authors and/or other copyright owners and it is a condition of accessing publications that users recognise and abide by the legal requirements associated with these rights.

Take down policy

If you believe that this document breaches copyright please contact us providing details, and we will remove access to the work immediately and investigate your claim.

1 **Artificially generated turbulence: A review of phycological nanocosm, microcosm, and**
2 **mesocosm experiments**

3
4 **Russell N. Arnott¹, Mehdi Cherif², Lee D. Bryant¹, Danielle J. Wain^{1,a,*}**

5
6 *¹Department of Architecture and Civil Engineering, University of Bath, UK; ²Department of*
7 *Ecology and Environmental Sciences, Umea University, Sweden*

8
9 *Corresponding author: danielle.wain@7lakesalliance.org

10 *^aCurrent affiliation: 7 Lakes Alliance, Belgrade Lakes, ME, USA*

11
12 **Abstract**

13
14 Building on a summary of how turbulence influences biological systems, we reviewed key
15 phytoplankton-turbulence laboratory experiments (after Peters and Redondo (1997) and
16 Peters and Marrasé (2000)) to provide a current overview of artificial-turbulence generation
17 methods and quantification techniques. This review found that most phytoplankton studies
18 using artificial turbulence feature some form of quantification of turbulence; it is
19 recommended to use turbulent dissipation rates (ϵ) for consistency with physical
20 oceanographic and limnological observations. Grid-generated turbulence is the dominant
21 method used to generate artificial turbulence with most experiments providing quantified ϵ
22 values. Couette cylinders are also commonly used due to the ease of quantification, albeit as
23 shear rates not ϵ . Dinoflagellates were the primary phytoplanktonic group studied due to their
24 propensity for forming harmful algal blooms (HAB) as well as their apparent sensitivity to
25 turbulence. This study found that a majority of experimental set-ups are made from acrylate

26 plastics that could emit toxins as these materials degrade under UV light. Furthermore, most
27 cosm systems studied were not sufficiently large to accommodate the full range of turbulent
28 length scales, omitting larger vertical overturns. Recognising that phytoplankton-turbulence
29 interactions are extremely complex, the continued promotion of more interdisciplinary
30 studies is recommended.

31

32 **Keywords:** phytoplankton, interactions, harmful algal blooms, dinoflagellates

33

34 **DECLARATIONS**

35 **Funding:** Funding for this work was provided by a UK Royal Society International
36 Exchange Grant IES\R3\170070 awarded to D. Wain and M. Cherif. We also acknowledge
37 the financial support of the Knut and Alice Wallenberg Foundation (d.nr. 2016.0083).

38

39 **Conflicts of Interest:** None

40

41 **Data Availability:** Not applicable

42

43 **Code Availability:** Not applicable

44

45

46

47 INTRODUCTION

48 Turbulence is a key physical characteristic of aquatic systems that has profound impacts
49 on phytoplankton population dynamics. Many early studies of these complex biological-
50 turbulence interactions (Figure 1) focussed upon the role of turbulence in homogeneously
51 redistributing phytoplankton species throughout the water column. Stably stratified water
52 columns typically promote positively buoyant species, allowing them to access increased
53 light levels and, in nearshore waters, nutrients trapped above the pycnocline associated with
54 catchment runoff. This scenario is vastly generalised and broadly characterised; additional
55 studies into the various biological-turbulence interactions have yielded a variety of complex
56 feedback mechanisms (Figure 1).

57 To understand this array of interconnected feedback mechanisms and accurately predict
58 how phytoplankton behave in a given environment, researchers frequently adopt one of two
59 approaches. The first is to model a general phytoplankton population using either a single,
60 idealised species (Ross and Sharples, 2007; Ross and Sharples, 2008) or a combination of
61 idealised species, e.g., positively buoyant dinoflagellates against negatively buoyant diatoms
62 (Huisman et al., 1999). The second approach is to artificially produce turbulence in a
63 mesocosm facility (hereafter referred to as a cosm to include facilities across an array of
64 sizes) and expose either a monoculture, a mixture of species, or a natural population to
65 varying levels of turbulence (Peters and Redondo, 1997). It is the latter that this review
66 focuses upon.

67 This review begins with an overview of biological-turbulence interactions, drawing upon
68 key studies to highlight the complex relationship between phytoplankton and turbulence. Best
69 practice is then discussed with regards to the experimental design of phytoplankton cosm
70 studies. Building upon this, the main methods of artificial turbulence generation (grids,
71 shaker tables, aeration and Couette cylinders are discussed and reviewed, with less-

72 commonly used methods included in Appendix 1. This review culminates with a discussion
73 of the different techniques used to quantify turbulence in cosm experiments, with lesser-used
74 techniques found in Appendix 2.

75 Note that this review is limited to studies involving phytoplankton in controlled
76 laboratory settings and, to this end, omits observations of natural systems as well as
77 biological-turbulence interaction studies on higher trophic organisms (e.g., zooplankton and
78 fish larvae). A total of 102 publications were used to complete this review. For publications
79 where more than one generation technique was used, these have been counted as separate (a
80 total of 8). For single experiments that yielded multiple publications (a total of 14), these
81 have been counted as a single study. A summary table of all publications used for this review
82 can be found in Appendix 3.

83

84 **Quantifying Turbulence in Aquatic Environments**

85 Most aquatic environments are turbulent flows comprised of eddies of varying size. As
86 a fluid is perturbed at the macroscale (e.g., by wind), the energy imparted to that fluid
87 cascades down from larger to increasingly smaller eddies until is it dissipated by the viscosity
88 of the water. When measuring turbulence, there are a number of different variables that can
89 be used to quantify the turbulent field. If we consider the rate at which the kinetic energy
90 dissipates due to viscous forcing (i.e., the rate of turbulence kinetic energy dissipation; ϵ), it is
91 possible to quantify turbulence.

92 It is also possible to quantify turbulence via velocity shear. As a fluid flows past a
93 surface, shear is generated as friction between the fluid and the surface causes a boundary
94 layer. This layer diffuses away from the surface, perpendicular to the direction of the flow. At
95 certain thresholds, the boundary layer can give way to vortex shedding as the flow switches
96 from laminar to turbulent. Within the remit of this review, shear is only used to quantify

97 turbulence in studies that make use of Couette cylinders where shear flow is used to generate
98 turbulence inside the cylinder. For laboratory measurements to be comparable with those in
99 the field, it is thus recommended that turbulence values are reported as ε in units of m^2/s^3 ,
100 which are the more commonly reported field units across disciplines.

101

102 **Study Aim**

103 This review builds upon the seminal work of Peters and Redondo (1997) and
104 incorporates literature from over the subsequent 20-plus years in order to ascertain best
105 practice when it comes to laboratory-based turbulence-generation studies. There is clearly the
106 need for greater standardisation across turbulence studies to facilitate easier and more direct
107 comparisons between studies. Peters and Redondo (1997) originally set out to “*spark more*
108 *interdisciplinary science*,” aiming to support biologists by introducing them to the world of
109 turbulence.

110 As well as discussing the various methods of generating turbulence (along with
111 accompanied mathematical principles), Peters and Redondo (1997) made a key discovery: ε
112 generated in laboratory experiments can commonly be up to orders of magnitude higher than
113 the average level of ε typically observed in the oceanic surface-mixed layer ($\varepsilon = 10^{-5} \text{ m}^2/\text{s}^3$).
114 Many of the “classic” papers on the effects of turbulence on phytoplankton growth (White,
115 1976; Pollinger and Zemel, 1981; Savidge, 1981) actually made no attempt to quantify the
116 levels of turbulence to which their phytoplankton populations were exposed. Thankfully, as
117 this study area developed over time, practitioners retrospectively quantified their
118 experiments; it is now standard to include estimates of ε and/or other turbulence quantities (
119 Table I).

120 From descriptions of laboratory set-ups, Peters and Marrasé (2000) estimated that the
121 level of ε in some experiments could have been as high as $0.23 \text{ m}^2/\text{s}^3$. Results from

122 experiments with exaggerated levels of turbulence may have water-quality applications such
 123 as artificial mixing in reservoirs and bathing water (Kirke, 2001; Visser et al., 2016).
 124 However, if the purpose of the experiment is to accurately model a biological-physical
 125 system that would occur in a natural aquatic system, then it is crucial for the experimental
 126 set-up to be as representative as possible of the real world. It is highly prudent to correctly
 127 quantify the level of turbulence generated prior to commencing a study to ensure that
 128 experimental conditions are representative of the environment being replicated.

129

130 *Table 1 - Comparison of the main turbulence-generation techniques taken from publications*
 131 *between 1953 to 2020 inclusive (n=102). As well as the number of publications associated*
 132 *with each technique, we also see the proportion of studies which include turbulence*
 133 *quantification. See also Figure 6 for a chronology of publications for different turbulence*
 134 *generation methods.*

Turbulence generation method	Quantified	Quantified Elsewhere	Unquantified	Total Studies
Aeration	1	3	7	11
Couette	15	3	0	18
Grid	29	2	1	32
Shaker	6	9	4	19
Other	14	1	6	21

135

136 **Biological-Turbulence Interactions**

137 Turbulence can have a profound influence on individual cells, specific species, and
 138 community composition in many ways. Most simply, high levels of turbulence can cause
 139 mechanical destruction by detaching flagella (Pollinger and Zemel, 1981), directly
 140 impacting motility. Turbulence also acts as a mechanism by which to homogenously
 141 distribute positively buoyant, motile species throughout a water column or to resuspend
 142 negatively buoyant, non-motile species; this directly impacts cell access to the photic layer
 143 and/or the light climate to which a cell is exposed (Kjørboe, 1993; Visser et al., 2016). Thus,
 144 the turbulent regime of a water body can have a profound impact on the phytoplankton

145 community composition with corresponding effects further along the food web. To this end,
146 turbulence has been seen to increase both predator-prey encounter rates (Rothschild and
147 Osborn, 1988) and contact rates between parasites and phytoplankton cell hosts (Llaveria et
148 al., 2010).

149 At the cell level, turbulence can impact cell growth via altering rates of nutrient uptake
150 and exposure to light. Phytoplankton cells uptake nutrients from the surrounding water via
151 diffusion; reduced flow at the cell surface causes the water surrounding the cell (i.e., the
152 concentration boundary layer) to become nutrient depleted (Prairie et al., 2012) and replete
153 with waste (Lazier and Mann, 1989; Kiørboe, 1993). Turbulent flows are seen to increase the
154 laminar shear across the cell surface, eroding the concentration boundary layer and causing a
155 corresponding increase in nutrient flux to the cell (Lazier and Mann, 1989; Kiørboe, 1993;
156 Arin et al., 2002; Peters et al., 2006). Conversely, turbulence can also reduce the rate of cell
157 division (Sullivan et al., 2003) with prolonged exposure to high turbulence intensities
158 resulting in increased cell mortality (White, 1976; Pollinger and Zemel, 1981). Even short-
159 duration, high-intensity turbulence applied at a specific time in the cell cycle can inhibit cell
160 division (Pollinger and Zemel, 1981). Turbulence can also induce the “flashing light effect”
161 (a.k.a., the light–dark cycle, intermittent illumination, light intensity fluctuation and/or
162 dynamic light condition;(Sato et al., 2010)) in cells. This phenomenon has been observed to
163 increase the photosynthetic efficiency in cultured species exposed to intermittent light
164 fluctuations (Laws et al., 1983; Grobbelaar, 1989) via a reduction in photoinhibition (Nedbal
165 et al., 1996) thought to be linked to the light fluctuations that a cell would be exposed to
166 within a turbulent environment.

167 Turbulence also can cause changes in cell morphology. For example, the dinoflagellate
168 *Ceratocorys horrida* Stein experienced a reduction in cell size and spine length in response to
169 high turbulent intensities, an adaptation postulated to allow cells to sink below the more

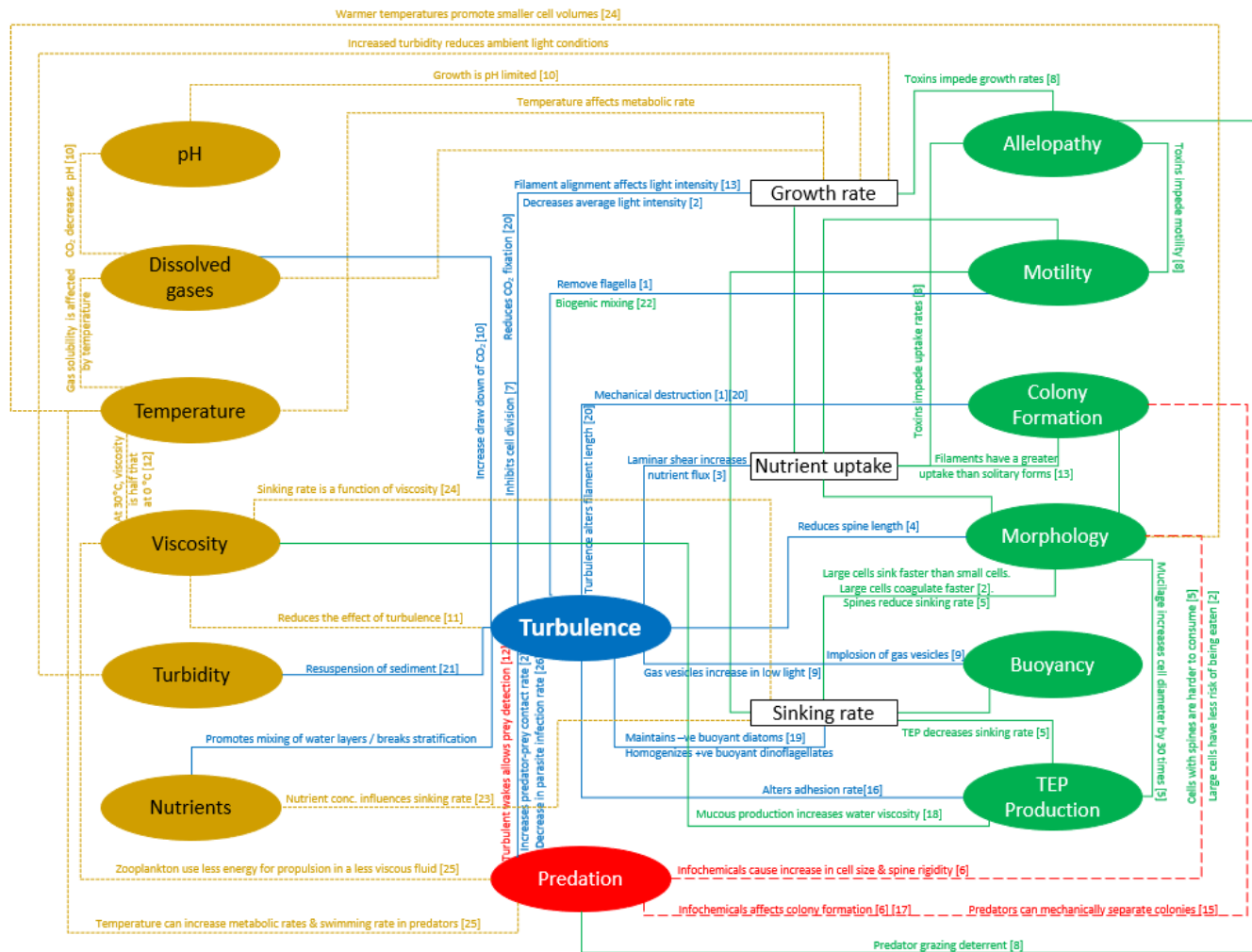
170 turbulent conditions and reduce risk of mechanical damage (Zirbel et al., 2000). Cell
171 morphology is also linked to light climate with elongated particles becoming aligned in the
172 direction of flow, thereby increasing the backscatter of light in the water column (Guasto et
173 al., 2012). Morphology is also linked to nutrient uptake, the rate of which preferentially
174 increasing in larger cells when compared to smaller cells in turbulent conditions (Guasto et
175 al., 2012).

176 Further studies linking turbulence to morphology and surface-area-to-volume (SAV)
177 ratios across different species suggested these parameters to be crucial in determining nutrient
178 uptake (Fraisse et al., 2015). Growth rate of large species was often exceeded by that of
179 smaller species in nutrient-limited conditions (Cózar and Echevarría, 2005) whereas shape
180 dictated how a species behaved hydrodynamically while in turbulent flows and whilst sinking
181 (Padisák et al., 2003). Clearly, shape and SAV ratios are interlinked; elongated cells were
182 seen to outcompete spherical cells with regards to nutrient acquisition (Pahlow et al., 1997).

183 Morphology also plays a key role in how colonial, chain-forming filamentous species
184 interact with turbulent fields; for example, longer filaments sink faster in calm conditions, but
185 under turbulent conditions a filament can grow to greater sizes as a result of turbulence-
186 induced increases in light access (Fraisse et al., 2015). Chain-forming, postulated to be a
187 means for avoiding grazing (Kjørboe, 1993), also provides a mechanism by which to increase
188 form drag and thereby reduce sedimentation (Padisák et al., 2003). Turbulence has been
189 observed to separate large colonies, thereby separating filament chains into smaller sections
190 (Pahlow et al., 1997) which are able to sink and access additional nutrients at depth (Padisák
191 et al., 2003). The ability of a colony to deform in different flow environments is thought to
192 give colonial species a competitive advantage in a wider range of turbulent regimes (Guasto
193 et al., 2012). Turbulence-enhanced nutrient uptake is also seen to preferentially affect
194 colonies when compared to singular cells (Guasto et al., 2012). Chain-forming species exhibit

195 a range of lengths, orientations and flexibilities, all of which affect their hydrodynamic
196 properties. Compared to flexible chains, increasingly stiffer chains not only exhibit higher
197 rates of nutrient consumption but also experience larger nutrient fluxes (Musielak et al.,
198 2009). With focus on phytoplankton as a carbon pump, colonial diatoms are known to be
199 prolific fixers of carbon dioxide (CO₂) where under turbulent conditions, they export carbon
200 from the upper ocean to depths by forming fast-sinking aggregates. To this end, rates of
201 turbulence-enhanced carbon uptake have been observed to be higher in chain-forming species
202 than in individual cells (Bergkvist et al., 2018).

203 The traditional view of phytoplankton behaving as benign passengers at the whims of
204 forces within the water column holds for macroscale flows; however, the various experiments
205 described within this review act to showcase a dynamic group of organisms capable of
206 complex abilities and feedback mechanisms permitting them to gain a foothold over
207 competing species by altering their properties to suit the conditions of the water column.
208 Increasingly, researchers are recognising that different phytoplankton have an array of
209 ecological adaptations that allow them to prosper within an array of various turbulent
210 environments (Margalef, 1997; Fraisse et al., 2015). With emphasis placed on the effect of
211 turbulence, Figure 1 allows us to appreciate the complexity of turbulence-plankton
212 interactions. Further weight is added herein to recommendations found in key papers
213 (Margalef, 1997; Peters and Redondo, 1997) which characterise turbulence within a water
214 column to be as significant a biological determinant as temperature or salinity, thereby
215 emphasising the importance of measuring shifts in phytoplankton communities and
216 turbulence concurrently.



- [1] Pahlow et al. (1997)
- [2] Kjørboe (1993)
- [3] Lazier and Mann (1989)
- [4] Zirbel et al. (2000)
- [5] Padisák et al. (2003)
- [6] Lürling (1998)
- [7] Pollinger and Zemel (1981)
- [8] Schwartz et al. (2016)
- [9] Walsby (1971)
- [10] Havskum and Hansen (2006)
- [11] Hellung-Larsen and Lyhne (1992)
- [12] Margalef (1997)
- [13] Guasto et al. (2012)
- [14] Leterme et al. (2008)
- [15] Dawidowicz (1990)
- [16] Beauvais et al. (2006)
- [17] Long et al. (2007)
- [18] Smayda and Reynolds (2001)
- [19] Huisman et al. (1999)
- [20] Moisander et al. (2002)
- [21] Visser et al. (2016)
- [22] Katija (2012)
- [23] Bienfang et al. (1982)
- [24] Naselli-Flores et al. (2020)
- [25] Simoncelli et al. (2019)
- [26] Llaveria et al. (2010)

Figure 1 - Flow diagram summarising various links and feedbacks of phytoplankton-turbulence interactions. Green = biological characteristics; white = rates; blue = turbulence processes; red = predation; gold = water properties. Associated coloured text denotes the forcing factor for that link. Where appropriate, links are qualified with numbered references. Dashed lines are included to assist colour-blind readers in distinguishing problematic colours.

217 **EXPERIMENTAL DESIGN**

218

219 **Facility Considerations**

220 Before evaluating different methods of turbulence generation, the experimental
221 vessel(s) itself should be considered as something as simple as the shape, scale and material
222 can considerably influence the experiment if not properly accounted for. As such, the
223 following section discusses the potential implications of tank volume, tank shape, the material
224 the tank is constructed from and how the tank is filled.

225

226 *Volume of Tank*

227 Crossland and La Point (1992) posed the question: “*How big does a mesocosm have to be to*
228 *provide a realistic simulation of the natural environment?*” The answer is very dependent on
229 the scale and scope of study taking place. Throughout the literature, however, the terms
230 nanocosm, microcosm and mesocosm are frequently used interchangeably. Whether a cosm is
231 classed as nano-, micro-, or meso- is open to interpretation with some using volume as the
232 distinguishing feature (Waller and Allen, 2008; Alexander et al., 2016) while others use
233 diameter or length (Kangas and Adey, 2008). In summary, Solomon and Hanson (2014)
234 provided the best characterisation of the different cosms (Table 2). Traditionally, researchers
235 used small (< 1L) nanocosms described as “simplified, physical models of an ecosystem that
236 enable controlled experiments to be conducted in the laboratory or in situ” (Matheson, 2008).
237 Increasing in size leads sequentially to microcosm and mesocosm systems, generally
238 described to be “bounded and partially enclosed outdoor experimental setups falling between
239 laboratory microcosms and the large, complex real world macrocosms” (Odum, 1984). These
240 facilities may be housed inside or outdoors (i.e., on land or in water) depending on the nature
241 of the setup. For outside enclosures suspended within an aquatic environment, Solomon and

242 *Table 2 - Characterisation of different cosms. After Solomon and Hanson (2014).*

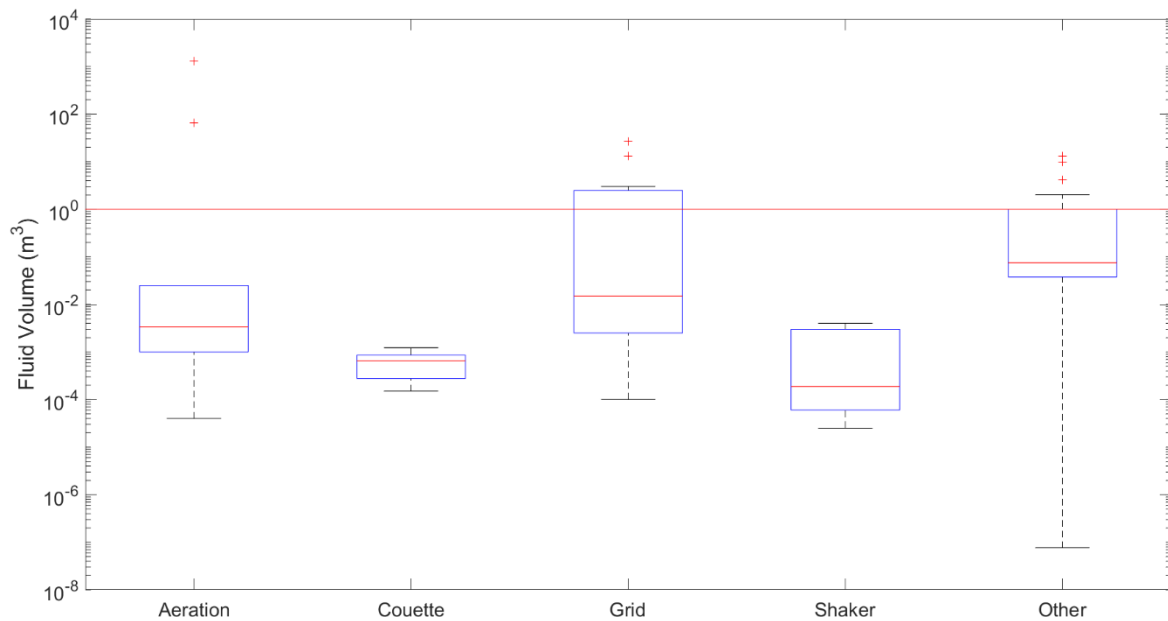
	Nanocosm	Microcosm	Mesocosm
Volume (L)	1 – 100	100 - 15000	>15000
No. of Trophic Levels	2	3+	3+
Optimum study duration	<8 weeks	<1 season	>1 season
Typical Location	Inside	Inside or outside	Outside

243

244 Hanson (2014) suggested the term ‘limnocorral’ to differentiate these from facilities on land
 245 while Parsons et al. (1978) opted for a controlled ecosystem enclosure.

246 With regards to biological studies, a larger experimental volume supports greater
 247 biodiversity and allows for a larger number of trophic levels to be observed concurrently
 248 (Alexander et al., 2016); conversely, smaller microcosms typically exclude higher trophic
 249 levels due to size constraints (Matheson, 2008). With regards to turbulence, vertical overturns
 250 are known to exist between 10^{-3} to 10^1 m; while smaller cosms represent the smaller end of
 251 this range, clearly a much larger tank would be required in order to capture the upper range.
 252 After all, it is not possible to produce a 10 m vertical overturn if the tank itself is shallower
 253 than 10 m depth. Using cosm volume as an indicator of maximum turbulent overturn size
 254 within a particular experiment, a majority of studies were found to use fluid volumes smaller
 255 than 1 m^3 (Figure 2). As expected, it is larger volume limnocorral studies that make up a bulk
 256 of the experiments above this 1 m^3 threshold.

257



258

259 *Figure 2 - Boxplots of approximate fluid volumes involved with different types of turbulence-*
 260 *generation experiments. Central line in each box is the median; top and bottom of each box*
 261 *indicate the 25th and 75th percentiles. Whiskers extend to the most extreme data points not*
 262 *considered outliers, with outliers plotted as plus-signs. Continuous horizontal line indicates a*
 263 *volume of 1 m³, considered to be the minimum volume required to capture realistic turbulence*
 264 *length scales Note the log scale on the y-axis.*
 265

266 *Shape of Tank*

267 Peters and Redondo (1997) put forth the assumption that biologists tend to use
 268 cylindrical tanks as, in theory, these display a higher degree of homogeneity. Conversely,
 269 physical studies are generally undertaken in cuboid tanks as the corners disrupt secondary
 270 flow effects; at the same time, modelling flow within square-based tanks is considered
 271 simpler mathematically. However, cuboid tanks are considered less homogenous overall due
 272 to the presence of corners (Peters and Redondo, 1997) which can cause 1) material to collect,
 273 2) organisms to grow there and/or 3) changes in the turbulent field. In a comparison between
 274 turbulence generated in smooth- and baffled-bottom flasks, ϵ values were seen to be two
 275 orders of magnitude higher in the latter (Kaku et al., 2006). The shape of a tank can clearly
 276 play a significant role in the turbulence regime within.

277 Matheson (2008) acknowledged the importance of SAV ratio in microcosm design;
278 those with a large SAV ratio can promote edge communities of biofilms or cause other
279 organisms to congregate to avoid predation. As such, these biological “wall effects” can add
280 significant bias into an experiment; efforts should hence be made to use facilities with small
281 SAV ratios. The size and aspect ratios of the test vessel would be expected to affect the
282 growth rate for many reasons. High-volume growth “ponds” (i.e., vessels with a shallow
283 depth but increased exposed water surface area) are designed to maintain as much of the
284 population in the photic layer as possible while also reducing the effects of shadowing. A
285 larger exposed water surface area would not only increase gas exchange across the boundary
286 but would also promote a higher evaporation rate.

287

288 *Material of Tank*

289 Vessels may be constructed out of an array of different materials depending on
290 availability and size requirements. Firstly, it is essential that the material of the tank does not
291 influence the fluid medium inside the tank. As such, it is not advised to use ferrous materials
292 to construct mesocosms as not only does this add iron to the fluid medium (which is a
293 photosynthesis-limiting micronutrient; (Martin and Michael Gordon, 1988) but the tank itself
294 is also at risk of corrosion, especially if using saline fluid media.

295 Other materials may also cause micronutrients to be leached into the culture medium;
296 glass has the potential to provide a source of silicon, known to be a limiting nutrient for
297 diatoms (Kilham, 1971). Hellung-Larsen and Lyhne (1992) studied the effects of vessel
298 material on the rates of cell division in the protozoan *Tetrahymena* sp. and observed no
299 significant difference when using glass, siliconized glass and plastic.

300 With an increasing propensity for ecologists and other researchers to experiment with
301 three-dimensional (3D) printing technology, it has been observed that certain extrusion

302 materials, particularly resins, remain toxic to aquatic organisms for some time. Should a
303 microcosm tank be 3D-printed in resin, however, exposure to ultraviolet (UV) light can
304 reduce its toxicity substantially (Behm et al., 2018).

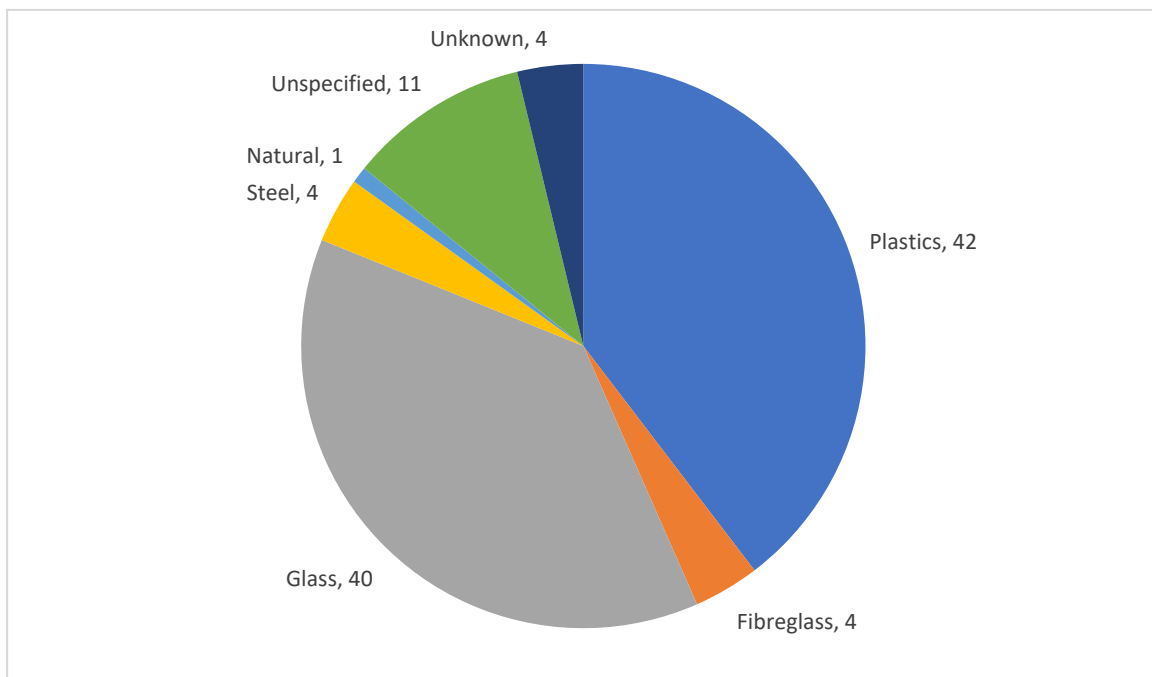
305 Conversely, many cosms are constructed from artificial polymers such as acrylate,
306 polyvinyl-chloride (PVC) and polycarbonate which all undergo photodegradation reactions
307 under UV light (Yousif and Haddad, 2013), potentially releasing toxins that could adversely
308 influence productivity. In a similar vein, the presence of polystyrene nanoplastics were seen
309 to reduce the chlorophyll content of the diatom *Chaetoceros neogracilis* VanLandingham
310 with subsequent implications on cellular growth and photosynthetic efficiency (Gonzalez-
311 Fernandez et al., 2019). As such, it is crucial that the tank material itself is not influencing the
312 growth rate of the organisms being studied. Some plastics are also permeable to certain gases;
313 depending on the nature of the study, this should also be considered and may even be
314 desirable (Matheson, 2008).

315 As well as releasing chemicals into tank water, certain cosm materials can absorb
316 chemical species from the water (Kangas and Adey, 2008). Zhou et al. (2016) submerged
317 Plexiglass tanks in water for 15 days prior to their experiment to allow the tanks to absorb
318 and/or release any chemicals and equilibrate accordingly. Of the cosms studied, a third was
319 comprised of plastics that undergo UV degradation (Figure 3). Another third was made of
320 glass which may be correlated to the high proportion of studies using glass Couette cylinders
321 and Pyrex vessels on shaker tables.

322 Typically, biologists cultivate cells in transparent vessels to maximise incident light
323 that allows cells to reproduce further. This eliminates any light gradient within the tank that
324 would be present in nature. As such, it is advised to use opaque materials when studying the
325 effects of turbulence; this generates a light-gradient through the tank which can have a
326 significant impact on results, especially when using phototactic or motile species or those

327 with the ability to regulate their buoyancy. It should also be noted that while surface shading
328 is a natural phenomenon that regulates phytoplankton growth, light introduced through
329 transparent walls is susceptible to biofilm growth resulting in decreased light levels over time
330 (Matheson, 2008). Some practitioners have avoided this effect via a periodic scrubbing of the
331 tank walls with a brush or similar (Zhou et al., 2016).

332



333

334 *Figure 3 - Materials used in cosm design (based on n=102 studies). Plastics refers to tanks*
335 *comprised of acylate, polycarbonate, polyethylene and polyvinyl chloride, all of which are*
336 *known to undergo UV degradation. Glass refers to both standard glass and Pyrex. For cosms*
337 *comprised of more than one material (n = 2), these materials have been counted separately.*
338

339 *Filling*

340 Phytoplankton-turbulence studies that use smaller nano- and microcosms typically
341 study the effects of one or two different species at a time based on seeding of the cosms with
342 laboratory-cultivated cells grown in incubators. However, larger mesocosms and limnocorrals
343 are typically used to look at natural planktonic communities that may be comprised of
344 multiple trophic levels and organisms of different sizes. Land-based facilities are typically
345 filled via pumping offshore waters from a particular depth into the enclosures (Båmstedt and

346 Larsson, 2018). Ideally, sets of cosms will be filled simultaneously or as close timed as
347 possible to insure homogeneity across all replicate cosms. It is important that the pump filling
348 system does not inadvertently preclude any larger species nor damage them in their transport
349 through the pump system (Striebel et al., 2013). Some facilities are able to filter certain size
350 fractions from the inflow water (Båmstedt and Larsson, 2018), thereby allowing e.g.,
351 microzooplankton through but omitting mesozooplankton that might graze upon certain size
352 fractions or cause morphological changes via infochemicals (Long et al., 2007; Figure 1).

353

354 **Environmental Variables**

355 Having evaluated potential issues that may arise within different facilities, we next
356 considered how environmental variables within the cosms may be influenced by particular
357 experimental setups. Specifically, we looked at the implications of study duration, nature of
358 the turbulence generated, light climate within the tank and general properties of the water
359 itself.

360

361 *Duration of study*

362 As suggested by Table 2, the duration of a study is somewhat dictated by the volume
363 of the tank, with larger facilities being able to accommodate a higher number of trophic levels
364 (Solomon and Hanson, 2014). It stands to reason that any change in the turbulent regime
365 within the tank will take time for its effects to cascade through a wider array of trophic
366 communities. Depending on the rate of cell division across different species (and given
367 conditions that promote or inhibit growth), it is expected that a phytoplanktonic community
368 would adjust to a new turbulent regime within a few days. Given a minimum cell division rate
369 of ~0.5 divisions per day (Banse, 1991), two days should account for cells to replicate at least
370 once.

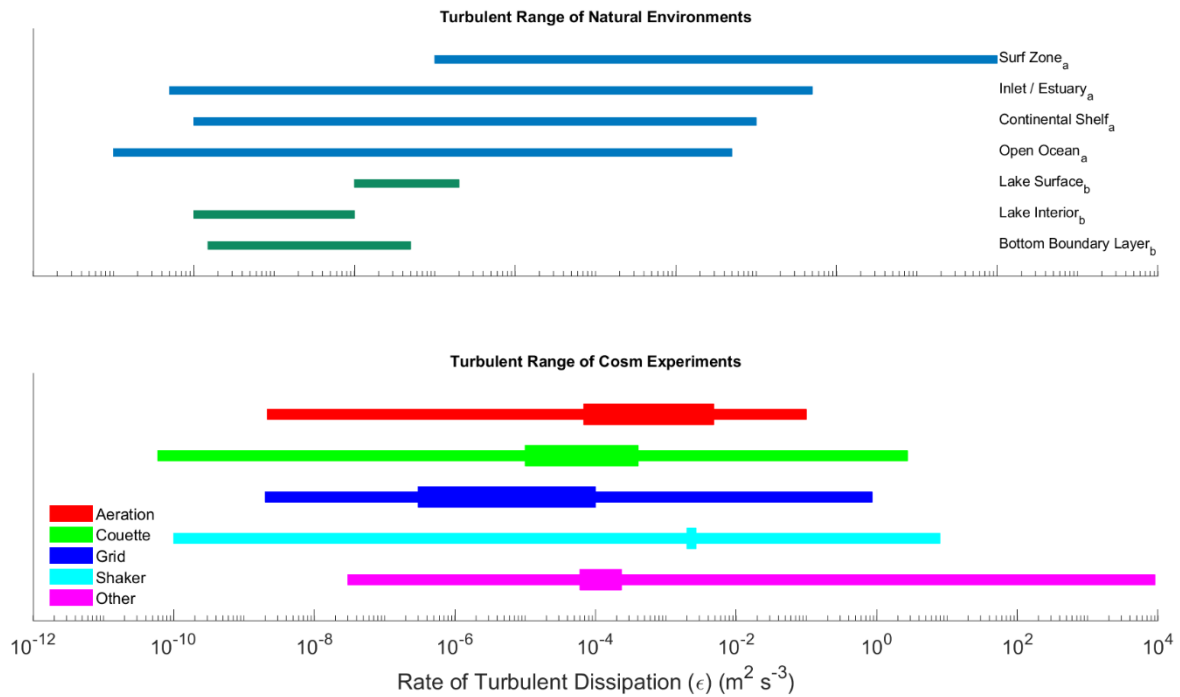
371 It is important to account for the effects of turbulence on growth due to changes in
372 light regime (Kjørboe, 1993), changes in cell division rate (Pollinger and Zemel, 1981) and
373 morphological changes to future generations (Zirbel et al., 2000). Once the new turbulent
374 regime is established and the community adjusts accordingly to the new physical
375 environment, ecological processes will dominate in regard to inter-species and trophic
376 interactions.

377

378 *Intensity or level of turbulence*

379 If the purpose of conducting laboratory experiments is to ascertain the effect(s) of
380 turbulence on a planktonic population, then it is crucial for the generated turbulence to
381 properly represent the real-world, naturally turbulent environment to which organisms would
382 be exposed. Using large, external limnocorrals may seem to be the easiest way to ensure that
383 the turbulence within a cosm is as natural as possible; however, it has been observed that
384 enclosing a portion of a water body within a cosm can significantly reduce the internal mixing
385 regime when compared to conditions immediately outside the enclosure (Striebel et al., 2013).

386 As well as the tendency to produce excessive and unrealistic levels of turbulence
387 within a cosm (Peters and Marrasé, 2000), there are a number of reasons to rethink existing
388 approaches to artificially generated turbulence. It is important to consider how turbulence
389 manifests itself within aquatic environments where turbulence is generally relatively weak.
390 Observations suggest that ϵ typically exists between 10^{-10} and 10^{-7} m^2/s^3 , both in central ocean
391 systems (Fuchs and Gerbi, 2016) and freshwater lakes (Wüest and Lorke, 2003). While wind-
392 mixed and convectively mixed surface layers seldom exceed 10^{-5} m^2/s^3 in the open ocean, surf
393 zone ϵ values of up to 10^{-2} m^2/s^3 have been observed (Fuchs and Gerbi, 2016). Of the
394 experiments reviewed here, a majority focused on the upper range of ϵ found in natural
395 environments (Figure 4).



396

397 *Figure 4 – Upper: comparison of range of turbulent dissipation rates (ϵ) found in marine and*
 398 *lacustrine environments taken from Fuchs and Gerbi (2016)(_a) and Wüest and Lorke*
 399 *(2003)(_b) respectively. Lower: ϵ produced from turbulence-generation studies evaluated for*
 400 *this review ($n = 102$). Horizontal lines span total ranges (thin lines) with the lower and upper*
 401 *log-median ϵ limits (thick lines) for each generation method.*
 402

403 In addition to being relatively weak, turbulence in natural environments can be highly
 404 sporadic, both temporally and spatially (Waterhouse et al., 2014). Thus, laboratory
 405 experiments that constantly force turbulence generation and aim for isotropic conditions
 406 across relatively small tank volumes are unrepresentative of natural conditions. In particular,
 407 direct and indirect turbulence avoidance strategies have been observed in planktonic
 408 organisms at a number of trophic levels (Franks, 2001; Pringle, 2007). Thus, for a cosm to
 409 properly represent the natural environment, a refuge region of less-turbulent water should be
 410 incorporated into the experimental design to allow the organisms some respite from intense
 411 turbulence and to facilitate natural behavior (Franks, 2001). It is thus recommended that
 412 experimental designs of cosms need to be large enough to include this refuge region. While
 413 this is thought to be particularly applicable to zooplankton studies, many motile

414 phytoplankton species position themselves within the water column to obtain light and/or
415 nutrients and would also benefit from tank refuge regions.

416

417 *Light*

418 Many standard biological growth facilities are designed to maximise growth with
419 regards to the light climate of the vessel. As mentioned previously, it is crucial for incident
420 light within turbulence-generation tanks to attenuate with depth. The biological-turbulence
421 interactions that underpin the critical depth hypothesis (Sverdrup, 1953) would be invalidated
422 if light-levels did not attenuate with depth.

423 With regards to the light spectrum that organisms are exposed to, it is best to use
424 direct sunlight to capture all spectrographic components of the sun at surface level. While this
425 will be the natural default in outdoor facilities and limnocorrals, indoor facilities traditionally
426 have relied on filament lamps that had a tendency to over-represent light within the infrared
427 parts of the spectrum, causing heating to the cosm surface and various thermal lid effects
428 (Båmstedt and Larsson, 2018). Conversely, filament lamps under-represent the UV
429 component of sunlight and, while UV light is attenuated quickly in the water column, it can
430 still have an influence on cosm ecology. For example, waters with high levels of coloured
431 dissolved organic matter (CDOM) have been shown to increase the attenuation of visible
432 light, thereby reducing the depth of the upper photic layer (Reynolds, 2009). CDOM
433 preferentially absorbs visible light towards the blue end of the spectrum as well as UV. The
434 UV light interacts with an array of complex compounds found in CDOM, causing them to
435 decompose into smaller compounds which can more easily interact with other biochemical
436 processes. Thus, the presence of CDOM in the water column can have a profound impact on
437 primary productivity with depth (Coble, 2007). Paczkowska et al. (2017) showed the explicit
438 link between CDOM and the phytoplanktonic community; as CDOM degrades in the

439 environment, it provides an important nutrient supply for heterotrophic bacteria which are a
440 potential food source for any mixotrophic species. Furthermore, under the restricted light
441 conditions associated with CDOM, phytoplankton respond by increasing the cellular
442 concentration of the photosynthetic pigments, including chlorophyll-*a*. These restricted light
443 conditions can also promote a shift towards species with smaller cell sizes (Paczkowska et al.,
444 2017).

445 With the advent of halogen and LED lights, it is now easier to reproduce the surface
446 sunlight spectrum within indoor cosms, accounting for UV, visible and infrared components
447 accordingly. Care should still be taken to measure the photoactive radiation (PAR) within the
448 cosm to ensure it is attenuating sufficiently with depth and is not too bright to cause photo-
449 inhibition of cells. As for the duration of light exposure, it is recommended that the day-night
450 cycle match that of the natural levels the organisms would experience. While a simple binary
451 on-off timer may be used to achieve this, it is better to include faders in the cosm facility
452 design to gradually increase or decrease light levels over the course of the day as they would
453 occur in nature.

454 Additionally, the potential for the turbulence-generation apparatus in a cosm to shade
455 the water below should be considered. Placing grids, paddles, impellers and similar structures
456 into a tank can decrease the amount of surficial light that reaches the bottom of cosm. This
457 was considered to be an issue in a study by Rijkeboer et al. (1990), who promptly replaced a
458 steel paddle with a transparent Perspex one to minimise this effect.

459

460 *Temperature and salinity*

461 As with light levels, it is also prudent to expose test organisms to temperatures and
462 salinities that they would ordinarily be subject to in natural aquatic environments. While
463 temperature has the ability to directly alter photosynthetic and respiration rates in

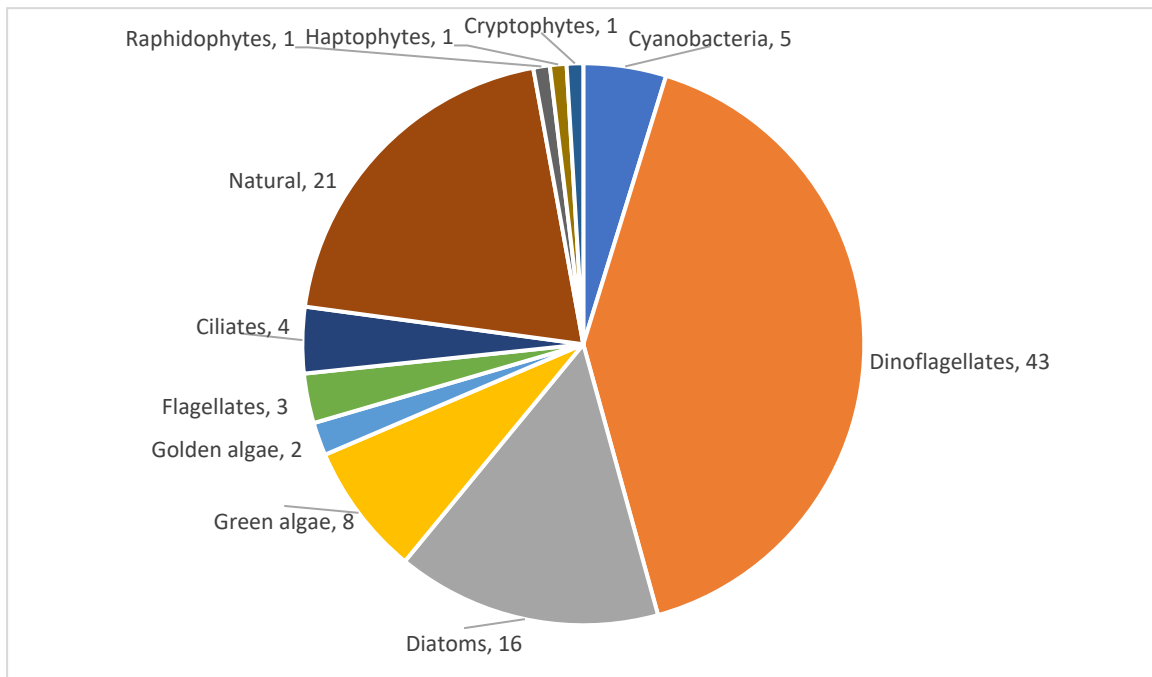
464 phytoplankton (Staeher and Sand-Jensen, 2006), there are also indirect temperature effects
465 including variations in the solubility of gases. Both temperature and salinity have an influence
466 on water viscosity which could affect microscale turbulence dynamics. In addition,
467 temperature has been found to be inversely related to cell volume (Naselli-Flores et al., 2020),
468 resulting in additional hydrodynamic variations that need to be considered.

469

470 **Biological considerations**

471 While smaller nano- and microcosm experiments lend themselves well to studying the
472 effect of turbulence on a single species, larger mesocosms can be used to investigate
473 interactions between two (or more) species (Havskum, 2003; Stoecker et al., 2006; Pannard et
474 al., 2007; Fraisse et al., 2015; Martínez et al., 2017). Due to their apparent sensitivity to
475 turbulence as well as their propensity to form harmful algal blooms, a majority of studies have
476 understandably focussed on the dinoflagellate group (Figure 5). Furthermore, this group
477 includes species with bioluminescent abilities; the light intensity emitted can be used as a
478 proxy for turbulent shear, thereby facilitating the quantification of shear in cosm experiments
479 (Stokes et al., 2004).

480 If using a natural planktonic population, it is possible to omit micro-zooplankton by
481 filtering the water used prior to filling the cosms (Båmstedt and Larsson, 2018). While this is
482 not suitable for predator-prey interaction studies, the removal of grazing should allow the
483 subtle impacts of turbulence interactions on the phytoplankton community to be more easily
484 observed. Choosing the correct filter to omit zooplankton grazers but not affect the larger size
485 fraction of phytoplankton can be difficult due to the overlap in sizes of these groups. It is also
486 likely that a natural phytoplankton population might contain mixotrophic ciliates and
487 dinoflagellates that graze on other species.



488

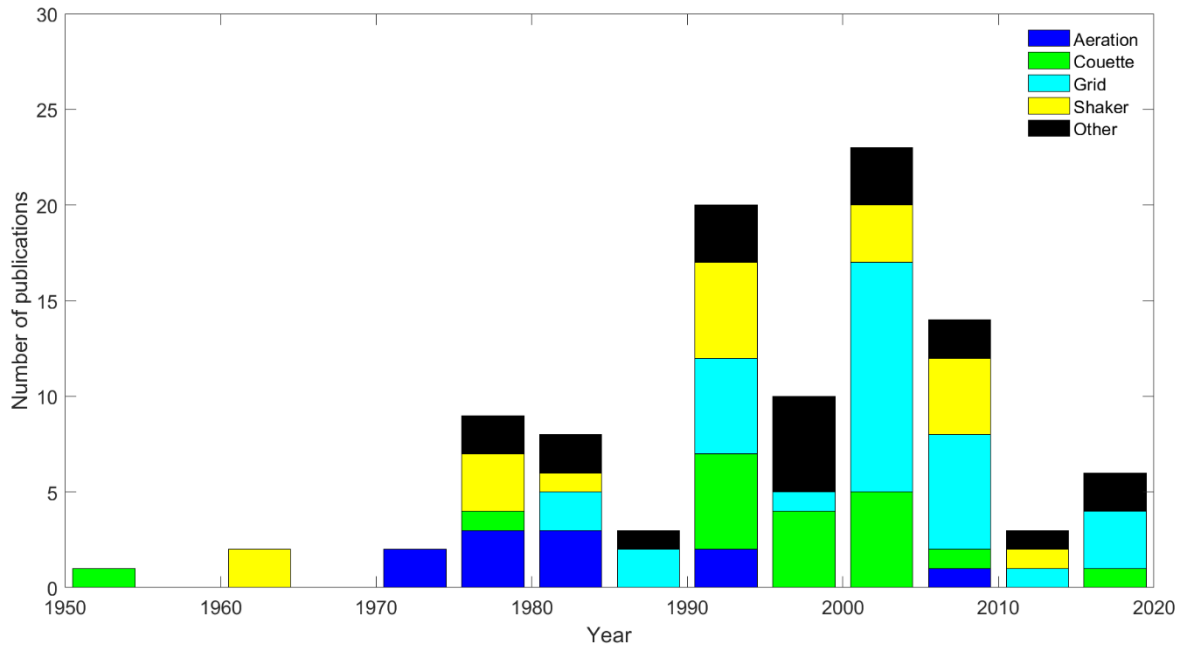
489 *Figure 5 - Proportion of different phytoplanktonic groups used in the evaluated turbulence-*
 490 *interaction experimental studies. Number of publications featuring that group is included next*
 491 *to each segment. "Natural" refers to experiments that made use of indigenous populations.*

492 **METHODS OF TURBULENCE GENERATION**

493 There are many ways to artificially generate turbulence in a laboratory environment;
 494 reviews of each of these different techniques and notable case studies for each are provided in
 495 this section. An analysis of previous methods identified that most studies use just four
 496 different methods: bubbling aeration, Couette cylinders, oscillating grids and laboratory
 497 shaker tables.

498 The chronology of publications (Figure 6) mirrors the information displayed in

499 Table 1; clearly grid-generated turbulence is the “industry favourite” with regards to
 500 phytoplankton-turbulence studies. Despite a boom in studies between 2000 and 2010, the
 501 recent decade has seen a decline of bio-turbulence publications; the lowest since the pre-
 502 1970s.



503

504 *Figure 6 – Stacked bar chart of phytoplankton-turbulence publications by year showing the*
 505 *proportion of different turbulence-generation techniques used.*

506

507 **Oscillating grids**

508 A standard way to generate turbulence within a tank is to use a grid mesh which is
 509 placed in the tank and connected to a mechanism that allows that grid to move through the
 510 water. This technique, referred to as “*a favourite in fluid dynamics experiments*” (Guadayol et
 511 al., 2009b) is often the preferred method of turbulence generation due to its simplicity as well
 512 as its established use in an extensive number of studies of this nature. Grids are typically of a
 513 similar width / diameter to the test tank and are a simple way to ensure a consistent turbulent
 514 field across the width of a tank. Typically, the grids are attached to a motor that allows them
 515 to oscillate vertically or horizontally at a given frequency and stroke length. A majority of
 516 these studies quantify ε (

517 Table 1; Figure 6) whereas early experiments simply used motor settings or revolutions-
 518 per-minute (rpm) as a proxy for turbulence intensity.

519 As with the tank material, the grid itself can be made from any material but it is
520 important that the grid does not corrode or deteriorate with time and remains biologically
521 inert. For this reason, the use of ferrous metals is discouraged as these materials will not only
522 degrade in saline water but will also provide a source of iron micro-nutrients. Netlon meshes
523 are typically used as they come in a variety of mesh-sizes and are hardwearing, easily
524 available, and corrosion-resistant. It is also possible to coat metal grids in inert substances
525 such as nylon (Savidge, 1981).

526 In a thorough comparison between turbulence generated by grids to orbital shakers,
527 Guadayol et al. (2009b) measured turbulence generated in a variety of different sized vessels
528 ranging from small 0.8 L nanocosms up to 2500 L microcosms. As well as tank size, different
529 grid configurations were trialled with variations in mesh size, bar width, grid diameter and
530 cross-sectional shape. Study results show that the turbulence generated using grids was
531 surprisingly isotropic (especially given the array of tanks size, grid dimensions and oscillation
532 speeds) but with the caveat that grid stroke length had to be comparable to the depth of the
533 tank. As such, Guadayol et al. (2009b) recommended using the maximum stroke length
534 possible in order to ensure isotropy.

535

536 *Vertically oscillating grids*

537 In order to mimic surface layer mixing, grids are typically suspended from the top of
538 the test tank. Grid nets can be singular (Savidge, 1981) or suspended in series of two or more
539 grids (Estrada et al., 1987; Alcaraz et al., 1988; Berdalet, 1992). There is also the option of
540 suspending an inclined, rotating ellipsoidal grid at a specific depth to promote mixing
541 horizontally as well as vertically (Estrada et al., 1987). While investigating an alternative
542 method to using grids, a number of disadvantages to using grid systems were identified by
543 Webster et al. (2004). Having an object moving through the study tank interferes with many

544 direct flow measurement techniques; however indirect techniques, such as particle tracking
545 velocimetry, can be readily used. Moving grids can also increase the likelihood of mechanical
546 damage to the study organism. In studies where the grid oscillates in only a small fraction of
547 the cosm, the turbulence field produced is non-isotropic and directional in accordance with
548 the direction of the grid motion. In this instance, the turbulence generated is also
549 heterogeneous as it decays with increasing distance from the grid. Webster et al. (2004) also
550 cited size, expense and complexity of apparatus as major disadvantages of grid systems; in
551 reality, however, a simple oscillating grid is vastly simpler than many other turbulence-
552 generation methods described herein. Furthermore, Warnars et al. (2006) recognised that
553 steep turbulence gradients are typically recorded with grid systems; ϵ is highest near the grid
554 but decays rapidly with distance from the grid. In addition, ancillary flows are seen to
555 accompany the primary flow field which exposes any test organisms to a wider range of
556 turbulent regimes than may be desired. Overall, Peters and Redondo (1997) discouraged the
557 use of oscillating grids on the grounds that the turbulence produced is not properly
558 representative of naturally occurring turbulence.

559 One disadvantage of grid systems is the steep turbulence gradients found around the
560 grid itself. If test organisms are permitted in and around the oscillating grid, they not only risk
561 mechanical destruction but are also exposed to a wider range of ϵ than they would in a natural
562 environment. To prevent organisms from interacting with the region of grid oscillation,
563 MacKenzie and Kiørboe (1995) used a fine mesh placed below the grid. The study focussed
564 on swimming behaviour and encounter rates between copepod larvae and cod / herring larvae;
565 thus, the barrier mesh size was selected to allow the prey copepods to interact with the grid
566 region while the fish larvae were unable to enter this region. The addition of the mesh screen
567 is a notable improvement to studies of this nature but could interfere with the turbulent field
568 produced by the oscillating grid. There is also the possibility that prey could pass through the

569 mesh screen where it could then be subjected to advantageous conditions for increased
570 growth. The presence of the screen could then prevent the now larger organism from passing
571 back through the mesh. In the case of phytoplanktonic studies with incident light from above,
572 this could provide an intrinsic bias to the study.

573

574 *Horizontally oscillating grids*

575 While most practitioners opt for vertically oscillating systems, there are times when a
576 horizontal system is more suitable. To reduce the likelihood of resuspension of filamentous
577 and dense species that sediment to the bottom, horizontal grids are better suited if using a
578 mixed phytoplankton community as shown in a study by Fraisse et al. (2015). Six different
579 phytoplankton species were selected to represent an array of morphologies (elongated shapes,
580 flattened shapes and motile species), densities, growth rates and sizes. The study showed that
581 the species selected that had high sinking rates were unable to outcompete those that could
582 maintain their positions in the upper column. Similarly, Schapira et al. (2006) made use of
583 horizontal grid systems taking care to produce both realistic and quantified turbulence
584 measurements. Opting for low, medium and upper limits of turbulence found in the English
585 Channel, the researchers investigated the impact of this on the colony-forming dinoflagellate
586 *Phaeocystis globosa* Scherffel. Results show that turbulence enhanced colony growth and
587 formation to a threshold amount after which turbulence was found to impede cell growth via a
588 postulated reduction in cell division (Schapira et al., 2006).

589

590 *Vibrating grids*

591 In addition to oscillating grids, vibrating grids have also been used; to study the effects
592 of turbulence on zooplankton behaviour, Saiz and Alcaraz (1992) utilised a vertically
593 orientated grid attached to a vibrating rod which moved the grid in the horizontal axes (x and

594 y). Efforts were made to not only quantify the turbulence generated but to also map the
595 turbulence field across the tank; it was found that the vertical and horizontal components of ε
596 did not differ to any significant extent. The results of the experiment showed that the increase
597 in turbulence caused a corresponding increase in both copepod suspension and predatory
598 feeding behaviour thought to result from an increase in predator-prey contact rates (Saiz and
599 Alcaraz, 1992).

600

601 *Stationary grids*

602 Looking to improve the often-used grid oscillation systems, Warnnaars et al. (2006)
603 used a pair of underwater speakers in anti-phase to push water through a stationary grid
604 placed directly in front of each speaker. It was observed that the flow characteristic of the
605 speaker system compared well with grid systems, albeit with lower strain rates making it
606 more representative of natural turbulence fields. Furthermore, ε is seen to attenuate rapidly
607 with distance from grids in oscillator set-ups; however, the speaker system generated
608 uniformly distributed ε throughout the entire volume of the tank. It is also noted that the range
609 of turbulence scales observed in grid systems is larger than those measured in the speaker
610 system; when the chlorophyte *Selenastrum capricornutum* Printz was exposed to the speaker
611 system, growth rate was seen to increase as conditions became more turbulent. This increase
612 in growth was attributed to the fact that the range of ε experienced by the organisms is more
613 concurrent with the levels in the natural environment. It should also be noted that in the
614 absence of a moving grid, this technique permits direct flow velocity measurements. Due to
615 limitations imposed by equipment practicalities, however, this technique would likely be
616 restricted to nanocosm and microcosm experiments.

617

618 *Additional case studies*

619 A number of researchers have used similar grid-generated turbulence set-ups to
620 observe predator-prey interactions within turbulent environments (Peters and Gross, 1994;
621 Peters et al., 2002; Dolan et al., 2003; Havskum, 2003; Havskum et al., 2005). For example,
622 Havskum (2003) investigated how grid-generated turbulence affected feeding rates of a
623 predatory dinoflagellate species linking turbulence to the rate of predator-prey interaction.
624 The disadvantage of studies of this nature is that, as well as altering the encounter rate, in
625 many cases the turbulence causes secondary physiological or behavioural changes in the
626 species studied (e.g., Peters and Gross (1994)). When conducting cosm experiments of this
627 nature, it is crucial to use planktonic species that are not sensitive to turbulence; for example,
628 Havskum et al. (2005) observed no change in the autotrophic or mixotrophic growth of the
629 dinoflagellate *Fragilidium subglobosum* (Stosch) Loeblich III under different turbulence
630 levels but did observe a change in ingestion rates.

631 In a technique analogous to grid-generated turbulence, Sullivan and Swift (2003) used
632 a pair of vertically oscillating rods to produce varied intensities of turbulence. Interestingly,
633 this paper opposed the commonly held view that dinoflagellates as a group are sensitive to
634 turbulence; out of the 10 species tested, 7 were unaffected by natural levels of turbulence. In a
635 similar departure from vertically oscillating grids, researchers at the Marine Ecosystem
636 Research Laboratory (MERL; Rhode Island, USA) mesocosms made use of a rubberised
637 plunger attached to a vertical pole to simulate tidal mixing. The plunger itself was situated 1m
638 above the sediment-laden floor to provide realistic levels of tidal sediment resuspension with
639 the system motor timed to providing a mixing cycle mirroring natural tidal oscillations
640 (Santschi, 1985).

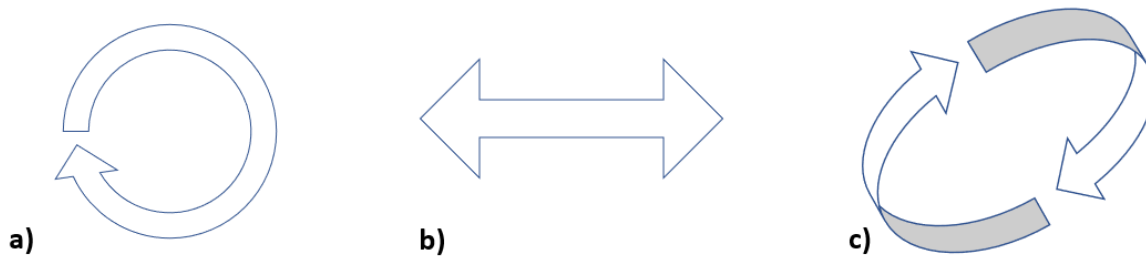
641 Towards the larger scale of mesocosm studies, it is also possible to use grid-generated
642 turbulence in limnocorrals (Nerheim et al., 2002). Studies undertaken as part of the Nutrients

643 and Pelagic Production project (Nejstgaard et al., 2001b; Nejstgaard et al., 2001a; Nerheim et
644 al., 2002) encountered difficulties with this approach, however. In order to promote
645 stratification in some of the limnocorrals, freshwater was added to the surface; this resulted in
646 the limnocorrals rising up out of the water as the mean internal water density was now lower
647 than that of the surrounding water. This effect was countered by increasing densities via the
648 addition of salt to the water in the lower parts of the mesocosms. Altering the salinity to this
649 extent in a biological study is not advised as this would alter the phytoplankton community in
650 favour of species that are less sensitive to changes in salinity. Once stratification was
651 established in the NAPP studies, the grid mixing systems were then used to promote an upper
652 mixed layer while a low-suction airlift pump system (typically used in aquaculture or marine
653 archaeology) promoted “slow circulation” in the upper layer.

654

655 **Shaker tables**

656 Shaker systems are used across a multitude of sciences for a variety of applications
657 from agitation of chemicals to the culturing of microbiological organisms. Due to the ubiquity
658 of shaker tables in academic and scientific institutions, it is not unsurprising that they are
659 frequently used to generate artificial turbulence. Furthermore, they typically have discrete
660 settings allowing researchers to generate a broad range of turbulence levels. While some
661 researchers simply use the rpm settings, more rigorous studies quantify the level of turbulence
662 via acoustic Doppler velocimetry or similar. It should be noted that specific turbulence flow
663 patterns generated by shaker tables are difficult to quantify, thus any recorded changes in
664 biological activity is difficult to ascribe to a particular flow characteristic (Warnaars et al.,
665 2006). Shaker tables typically use one of three different motion paths depending on their
666 intended application: orbital or rotary shakers; reciprocal shakers; and, gyratory shakers
667 (Figure 7).



669

670 *Figure 7 - Motion paths of vessels placed on different types of shaker tables as seen from*
 671 *above. a) An orbital / rotary shaker oscillates in a circular motion in the x-y plane. b) A*
 672 *reciprocal shaker oscillates from side to side along a single axis. c) A gyrotory shaker*
 673 *oscillates vessels in a circular motion with both horizontal and vertical components to the*
 674 *motion.*
 675

676 *Orbital shakers*

677 Orbital shakers (a.k.a. rotary shakers) agitate cultures with a circular motion in the x-y
 678 plane (Figure 7a). Depending on the manufacturer of the shaker, the orbit oscillation is fixed
 679 at a set distance or can be altered accordingly. Zirbel et al. (2000) used orbital shakers to
 680 observe changes in dinoflagellate morphology over time. Trials were conducted with the
 681 shakers set on 40 rpm to 120 rpm before a rate of 75 rpm was designated as “*relatively mild*”
 682 turbulence. It is noted that for such shaker experiments, turbulence occurs due to wall effects
 683 within the vessel. This has two ramifications: firstly, the turbulence will increase with
 684 proximity to the vessel walls and secondly, the vessel needs to be of a suitable size to allow
 685 turbulent mixing to impact upon fluid in the centre (Peters and Redondo, 1997). Orbital
 686 shakers typically promote the central “*doldrum,*” or dead-space, region in flasks marked by
 687 minimal in situ turbulence meaning that the cells are no longer being cultivated under near-
 688 isotropic conditions (Juhl et al., 2000). Furthermore, the turbulent mixing produced would be
 689 predominantly horizontal with a weak secondary vertical component. However, horizontal
 690 eddy diffusivity in the ocean is thought to be “*several orders of magnitude*” greater than the
 691 vertical equivalent (Okubo (1976) cited in Estrada et al. (1987)).

692 As shaker table experiments typically make use of available apparatus, there is often a
693 range of different sized and shaped vessels used which makes comparisons between studies
694 difficult. In a comparative study between turbulence generated by grids versus that generated
695 by orbital shakers, Guadayol et al. (2009b) trialled a number of different shaker set-ups with
696 different periods of oscillations as well as various volumes and flask (Florence, Nalgene and
697 Erlenmeyer) types. The research showed that at high levels of shaking, the turbulence field
698 remains isotropic independent of volume or flask shape. However, at lower levels of ε ($< 10^{-8}$
699 m^2/s^3), the isotropy began to fall, probably as a result of lower signal-to-noise ratios (SNR) in
700 the Doppler velocimeter as well as the fluid approaching the laminar-turbulent transition
701 point. Furthermore, orbital frequencies of < 1 Hz are not recommended as it is at approximately
702 this frequency that the laminar-turbulent transition occurs in flasks. As orbital shaker
703 turbulence is generated via wall friction, ε decreases with distance from the sides and bottom;
704 an order of magnitude decrease in ε was observed in measurements when transitioning from
705 the wall to the centre of the flask. Thus, it is recommended that “*small and narrow*” vessels
706 (e.g. Nalgene flasks) be used to limit this effect as much as possible (Guadayol et al., 2009b).

707

708 *Reciprocal shakers*

709 Reciprocal shakers oscillate from side to side along a single axis in the x- or y-plane
710 (Figure 7b). The length along which the oscillation occurs can be altered accordingly with
711 longer lengths equating to higher levels of turbulence (Juhl et al., 2000). The advantage of
712 reciprocal shakers is the removal of the central doldrum in the flasks which typically occurs in
713 orbital shakers. In a comparative study of the effects of shaker-table-generated mixing relative
714 to Couette-generated shear flow, Juhl et al. (2000) subjected populations of the dinoflagellate
715 *Lingulodinium polyedra* (F. Stein) J.D. Dodge to different durations of constant mixing.
716 Actually, reciprocal tables allow standing waves to form in the flask, resulting in an

717 oscillating fluid surface that ensures all cells in the population experience variable mixing.
718 While the level of turbulence was not quantified directly, attempts were made to approximate
719 mixing via a comparison of the qualitative outcome between the shaker populations and the
720 Couette populations; the response of the cells exhibited a similar response in both setups.

721

722 *Gyratory shakers*

723 As well as orbital shakers and reciprocal shakers, there are also gyratory shakers
724 which oscillate vessels in a circular motion with both horizontal and vertical components to
725 the motion (Figure 7c). An experiment was carried out to observe effects of gyratory-shaker-
726 generated turbulence (as well as of growth medium, fluid depth, tank material and initial cell
727 concentration) on the doubling time of the protozoan *Tetrahymena* sp. (Hellung-Larsen and
728 Lyhne, 1992). It was noted that gyrational shaking resulted in a circular wave that propagated
729 around the edge of the shaking vessel. The study showed that the doubling time was increased
730 (i.e., cell division decreased) with shaking but the impact of the shaking reduced with
731 increased fluid depth. Morphologically, cells that were exposed to shaking exhibited less-
732 prominent nuclear membranes and the development of small granules inside the cell
733 cytoplasm. It was also observed that viscosity played a role as the effect of shaking on cell
734 division was reduced when dextrane was added to increase the viscosity of the medium;
735 clearly, the increase in viscosity acted to reduce the overall level of turbulence in the vessels.
736 The study also compared the impact of gyratory agitation to reciprocal shaking and bubbling;
737 when using gyrational shaking, the impact of shaking rate on cell division was seen to be
738 dependent on initial cell concentration, but this was not so for reciprocal shakers
739 (Hellung-Larsen and Lyhne, 1992).

740

741 *Additional case studies*

742 Building upon early work regarding the mass culture of algae, Fogg and Than-Tun
743 (1960) used a shaker apparatus to ascertain the optimum shaking speed to maximise cultures
744 of *Anabaena cylindrica* Lemmermann. Even low agitation speeds were seen to increase cell
745 growth compared to unshaken cultures. While moderate shaking was seen to increase growth
746 due to increased suspension and nutrient flux, if the shaking rate exceeded 140 rpm, the cell
747 growth rate showed no increase when compared to unshaken cultures. Opposing these
748 findings, Tuttle and Loeblich (1975) attempted to find the optimal growth conditions for the
749 dinoflagellate *Cryptocodinium cohnii* (Seligo) Chatton and observed exponential death rates
750 of cells at both 40 and 80 rpm; these early results hinted at the turbulence sensitivity of some
751 dinoflagellate species.

752 In what has now become a classic paper in the study of phytoplankton-turbulence
753 interaction, White (1976) used rotary shakers to agitate cultures of *Alexandrium tamarense*
754 (Lebour) Balech to note the effect on cell growth while investigating the cause of red tides in
755 Eastern Canada. Results show that cell growth reduced rapidly at high levels of continuous
756 shaking; even intermittent shaking and/or shaking at low speeds was seen to adversely affect
757 cell growth. As well as mechanical destruction, White (1976) attributed the decreased growth
758 rate to cell disorientation that caused subsequent interference with phototactic migration.
759 Peters and Marrasé (2000) have since estimated the turbulence generated in this study to be
760 higher than natural ε with values between 4.30×10^{-3} and $1.19 \times 10^{-2} \text{ m}^2/\text{s}^3$. While the White
761 (1976) study made no attempt at turbulence quantification (it was, after all, at the time seen as
762 a purely biological study), it none-the-less sparked interest in turbulence studies within the
763 marine ecological community.

764 Clearly drawing upon these findings, Berdalet (1992) sought to identify the
765 mechanism(s) by which cell growth is reduced in turbulence. Cultures of the HAB

766 dinoflagellate *Akashiwo sanguinea* (K. Hirasaka) Gert Hansen & Moestrup were exposed to
767 shaker-table turbulence with cellular volume, shape and location of nuclei, RNA and DNA
768 concentrations all recorded. Berdalet (1992) postulated that the observed reduction in growth
769 was a result of the physical disruption of chromosome separation during cell division. Again ε
770 was unquantified in this study (Peters and Marrasé (2000) later estimated the corresponding ε
771 as $2 \times 10^{-3} \text{ m}^2/\text{s}^3$), but more recent studies based on the same experimental set-up utilised an
772 acoustic Doppler velocimeter to record water speed at different points in the flask (Berdalet et
773 al., 2007). Of relevance within the current review is a thorough literature overview of all
774 experiments on turbulence-dinoflagellate interactions which, as per Peters and Marrasé
775 (2000), includes estimates for ε calculated using experimental set-up data from individual
776 experiments (see Appendix 3).

777

778 **Aeration systems**

779 When biologists look to cultivate cells, they often seek to aerate the water via a bubble
780 stone at the base of the tank which allows gases (e.g., CO₂, oxygen) to diffuse into the water,
781 promoting growth. As such, bubble plumes and aeration systems in the lab are a tried and
782 tested technique for mixing water and aerating growth tanks. Furthermore, most
783 microbiological laboratories have access to air compressors and piping to facilitate the use of
784 aeration systems. A by-product of this aeration is that the bubbles themselves break down any
785 stratification, thereby homogenising the water while also advecting the cells as the central
786 bubble plume effectively promotes formation of a toroidal convection cell in the tank. Within
787 the mesocosm community, aeration systems are typically seen to be gentler in their approach
788 to turbulence generation due to their absence of moving parts that have the potential to
789 mechanically damage organisms (Sanford, 1997; Striebel et al., 2013).

790 In laboratory setups, it can be difficult to determine whether the change in growth rate is
791 a result of the turbulence induced by the bubble flow or as a result of atmospheric gases being
792 entrained through the water. How the culture will react is species-dependent with dissolved
793 oxygen being required for respiration while CO₂ promotes photosynthesis. Gas addition can
794 also result in a change in pH via CO₂-induced decreases in the pH of water; this can have
795 impacts for pH-sensitive species (Havskum and Hansen, 2006). An unintended side-effect of
796 bubbler aeration systems is a temperature change to the fluid medium. As gases that are
797 introduced to the fluid are typically at air temperature, this can impart additional thermal
798 energy to the system. Furthermore, as the gas has typically undergone pressurisation prior to
799 release, there may also be associated adiabatic thermal effects.

800 Båmstedt and Larsson (2018) noticed an aggregation of bacteria, algae and detritus at
801 the water surface of their unmixed cosms during experiments. This was thought to be the
802 result of surface heating from the overhead irradiance lamps causing a thermal lid effect in the
803 upper 60 cm. It was found that bubbling at a rate of 1 Hz from 2 cm depth was sufficient to
804 break up the surface aggregation, but some mixing was required to break the thermal lid. As
805 such, a comparison between bubbling and surface mixing using fans angled at 45° to the
806 surface was carried out; overall fan mixing was found to mix the mesocosm faster than
807 bubbling. It should be taken into consideration that the bubbler system was set to emit a single
808 18 mm-diameter bubble at 1 Hz so as to not cause any undesirable aeration effects.

809 In an attempt to determine the optimal conditions for cultivating the dinoflagellate
810 *Cryptothecodinium cohnii*, Tuttle and Loeblich (1975) subjected cultures of cells to agitation by
811 aeration (as well as magnetic stirrers and shaker tables). Sterilized air was bubbled through
812 the medium at a rate of 1.8 L/min; the increase in observed growth rate was negligible. In a
813 series of experiments exploring potential biomass species, Thomas et al. (1984a); Thomas et
814 al. (1984b); Thomas et al. (1984c) used aeration systems to “vigorously” aerate and mix the

815 cell cultures. Using a gas mix of 1% CO₂ in air, two aeration pipes were placed at the bottom
816 of the tank and gas supplied at a rate of 2000 ml/min. The researchers reported “very high
817 densities” and reported no evidence of mechanical damaging of the cells despite the high
818 aeration rate. There was no control tank setup nor any attempt to quantify the turbulence
819 produced. Again, with reference to the commercial cultivation of phytoplankton, Aguilera et
820 al. (1994) used bubbler agitation in chemostats to mix cultures of a microalga. Novel in this
821 experiment was an attempt to quantify mixing in terms of mechanical energy supplied to the
822 system calculated using standard physical equations relating gas pressure, velocity, and the
823 conservation of mass and/or energy. Within this work, the role of turbulence was recognised
824 in preventing sedimentation, promoting a homogenous distribution of cells and nutrients, and
825 increasing the nutrient supply to the surface of the cell. However, agitation by bubbles was
826 also cited as a way by which gases are more efficiently diffused into the medium. As
827 discussed earlier, this effect of increased gas diffusion on cell growth would be difficult to
828 distinguish from changes due to the increase in turbulence.

829 Aeration systems have been used to good effect for studying natural planktonic
830 communities (Eppley et al., 1978; Sonntag and Parsons, 1979). As part of the Controlled
831 Ecosystem Pollution Experiment (CEPEX), Sonntag and Parsons (1979) used aeration to
832 simulate upwelling, then added salmonids to create an additional trophic layer that would
833 ordinarily be absent (the enclosures were taken to depth by divers and then slowly raised so
834 any suitably motile organism would have been able to escape). The study recorded high rates
835 of phytoplankton sedimentation suggesting that the aeration regime chosen was insufficient to
836 promote resuspension. Using the same limnocorrals, Nerheim et al. (2002) combined grid-
837 generated turbulence with an aeration system to study a natural food web. Researchers
838 quantified the rate of vertical mixing via a dye dispersion study; this led them to realise that
839 the vertical eddy diffusivity was 0.06 cm²/s, lower than the expected value outside of the

840 enclosures (Steele et al., 1977). It was thus postulated that the presence of the enclosures
841 reduced the horizontal mixing and as this is coupled to vertical mixing, there was a
842 subsequent impact on vertical mixing also. Efforts were made to limit daily mixing to the
843 level just required to break any measured stratification; however, no efforts were made to
844 quantify this vertical mixing. Microscopic analysis of the species within the enclosures
845 verified that the bubbles did not damage cells mechanically, with Eppley et al. (1978)
846 reporting “no grossly unnatural results”.

847

848 **Couette cylinders**

849 Named after French physicist Maurice Couette who first used them in 1890 (Couette,
850 1890), this equipment generates shear flow in a small gap between two concentric cylinders.
851 A fluid medium is placed in the gap between the smaller inner cylinder and the larger outer
852 cylinder. The inner cylinder then rotates at a given speed producing uniform flow conditions
853 (Peters and Redondo, 1997; Sullivan and Swift, 2003). A key advantage of this setup is that
854 shear flow can be easily calculated from angular velocity, thereby removing the need for
855 physical measurements to calculate flow parameters. Furthermore, a variety of different forms
856 of turbulence can be produced by rotating the cylinders at different velocities relative to each
857 other. However, Sullivan and Swift (2003) reported that the turbulence produced by Couette
858 cylinders is intrinsically unrepresentative of natural turbulence because it applies constant
859 shear both temporally and spatially.

860 Some of the first phytoplankton-turbulence studies were carried out using Couette
861 cylinders. Pasciak and Gavis (1975) conducted a series of experiments on the effect of
862 turbulence on nutrient uptake rate in diatoms. Interestingly, they compared the uptake rate
863 between cell cultures on orbital shaker tables to those inside a Couette flow. While the shear
864 flow rate was calculated for the Couette flow, no attempt was made to quantify the turbulence

865 generated inside the flasks on the shaker table. Building upon this work, Thomas and Gibson
866 (1990a,b) used an almost identical set-up to observe the impact of shear flow on nutrient
867 uptake on *Lingulodinium polyedra*, a HAB-forming dinoflagellate species. Using a series of
868 Couette cylinders with rotational speeds ranging from 1 rpm up to 60 rpm, the researchers
869 calculated various turbulent parameters using the rotational speed.

870 Using a similar Couette set-up, Juhl et al. (2000) also conducted an investigation on
871 the dinoflagellate, *Lingulodinium polyedra*. The aim of this experiment was to account for the
872 variability in studies by measuring the effect of turbulence on population growth under
873 varying light-dark cycles, differing light levels and different stages of the cell cycle. The
874 outcomes highlighted a number of key mechanisms: a) that cell growth rate decreased more
875 when flow was applied in the last hour of the dark phase as compared to applying it to
876 illuminated cultures; b) populations cultured in lower light conditions experienced
877 proportionately lower growth rates when exposed to flow than those cultured in higher light
878 conditions and c) older cultures in the late exponential phase experience higher mortality
879 under flow than cells in the early phase. A key outcome of this study was that the extent to
880 which turbulence affects the cell population is not only light-dependent but also depends on
881 the physiological state of the cell (and the phase of its life cycle).

882 Juhl et al. (2000) also compared the outcomes of the Couette studies to equivalents carried out
883 using turbulence generated using shaker tables. Unfortunately, the shaker table turbulence
884 was unquantified; however, attempts were made to approximate the shear flow via a
885 qualitative comparison of results. It should be noted that Warnars et al. (2006) recognised
886 that the minimum strain rate used in the studies of Thomas and Gibson (1990a,b) were up to
887 two orders of magnitude greater than those observed in the natural environment.

888

889 A summary of turbulence generation methods and associated advantages and
 890 disadvantages can be found in Table 3, along with example references highlighting best
 891 practice for each of the main techniques. Based on this review, it is recommended that
 892 oscillating grids become the turbulence-generation standard; of the techniques evaluated, the
 893 grid-generated turbulence is closest to that found in natural systems. Furthermore, it is
 894 relatively easy to adjust the experimental set-up in order to facilitate species across different
 895 groups and, on a broader topic scale, across the different marine science sub-disciplines. This
 896 technique is also the most commonly used (

897 Table 1), thereby facilitating easy comparisons with any future study. See Appendix 1
 898 for a summary of lesser-used techniques for generating turbulence including pumping,
 899 magnetic stirrers, rotating chambers, wave tanks, impellers / propellers, paddles, dialysis
 900 cylinders and convective mixing.

901

902 *Table 3 - Summary table of commonly used turbulence generation techniques*

Technique	Pro	Con	Example
Oscillating Grids	<ul style="list-style-type: none"> • Can be configured for near-isotropic turbulence • Reduction in resuspension (horizontal grids) • Can use mesh screens to create refuge area 	<ul style="list-style-type: none"> • Obstructs flow velocity measurement equipment • Risk of mechanical damage to organisms • Steep turbulence gradients; ϵ highest near grid but decays rapidly with distance 	Schapira et al. (2006)
Shaker tables	<ul style="list-style-type: none"> • Low-cost, off-the-shelf equipment • Commonly found in laboratories 	<ul style="list-style-type: none"> • Typically restricted to small volumes • Turbulence generated is non-isotropic with high ϵ near flask wall decreasing towards centre 	Berdalet et al. (2007)
Aeration systems	<ul style="list-style-type: none"> • Can be applied across all scales of cosm • Commonly found in microbiological laboratories 	<ul style="list-style-type: none"> • Introduction of gases causing secondary growth effects in cells • Bubbles can cause adiabatic thermal effects and impede flow velocity measurements 	Aguilera et al. (1994)

	<ul style="list-style-type: none"> • Possible to use equations to estimate turbulence from energy input 	<ul style="list-style-type: none"> • Not quantifiable turbulence 	
Couette cylinders	<ul style="list-style-type: none"> • Shear flow can be calculated from angular velocity, removing the need for physical measurements 	<ul style="list-style-type: none"> • Turbulence unrepresentative of natural systems 	Stoecker et al. (2006)

903

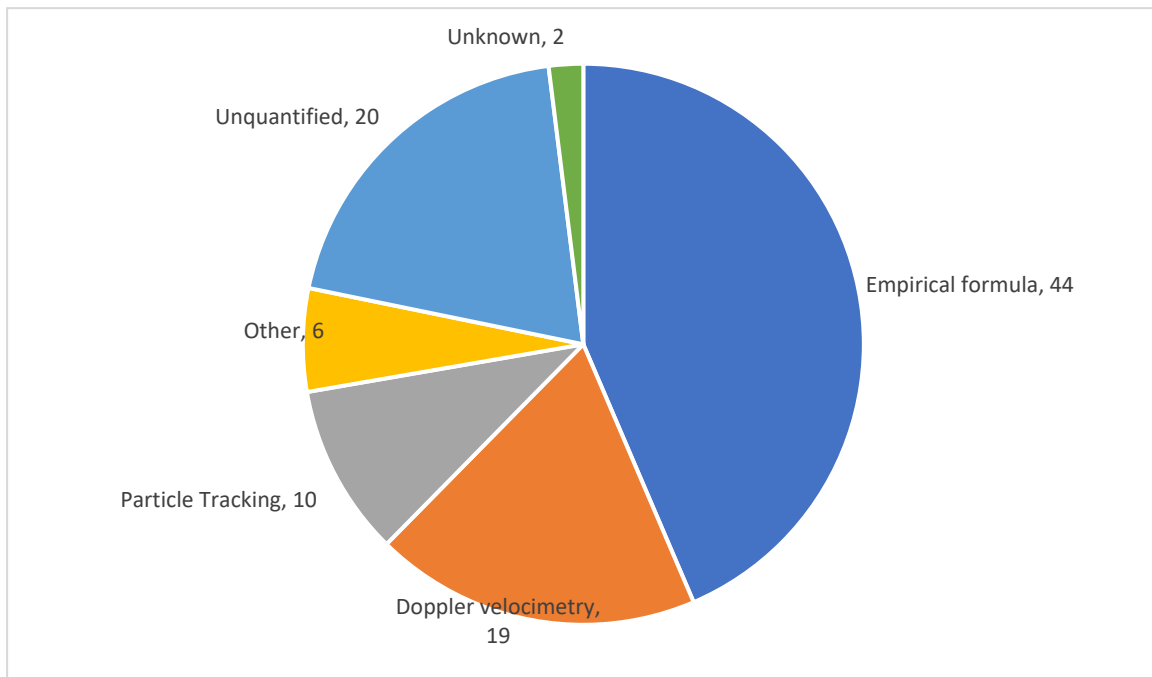
904

905 **METHODS FOR QUANTIFYING TURBULENCE**

906 It is crucial to properly describe the nature and quantify the magnitude of the turbulent
907 environment within a cosm. To relate a cosm experiment back to its intended real-world
908 application, organisms should be exposed to turbulence that mirrors natural turbulence as
909 closely as possible. While some studies simply use the rate of motor revolutions as a proxy
910 for turbulence quantification, others use an array of techniques to maintain turbulence
911 requirements. It should be noted that a majority of turbulence-generation techniques involve
912 the placement of movement apparatus in the test tanks (e.g., grids); as a result, it becomes
913 difficult to place sensors for turbulence measurement undisturbed in the tank as well.

914 Instead of measuring turbulence directly, some researchers simply consider the
915 mechanical energy input to the cosm (Kiørboe et al., 1990; Aguilera et al., 1994; Martínez et
916 al., 2017). For example, in a grid-generated turbulence study, Kiørboe et al. (1990) was able
917 to calculate ε as a function of power input from the motor as $\varepsilon = W/V \times 1/\rho$, where $W =$
918 power input (W), $V =$ volume of fluid (m^3) and $\rho =$ density of fluid (kg/m^3). While easily
919 calculated, these values are often theoretical and can be presented without proper calibration.
920 Given the ad hoc nature of many turbulence experiments, this estimate of ε (and associated
921 calibration) must be considered on a case-by-case basis (Guadayol et al., 2009b).
922 Furthermore, it also makes comparison between different studies difficult as this ε value is not
923 standardised nor easily comparable to natural systems.

924 The following section provides an overview to the various techniques used to quantify
925 turbulence as well as any corresponding advantages and/or disadvantages. Methods reviewed
926 include particle tracking velocimetry, particle imaging velocimetry, planar laser induced
927 fluorescence, Doppler velocimetry, and calculation via empirical formulae. Figure 8 shows a
928 breakdown of how frequently various methods have been used for turbulence quantification.
929



930

931 *Figure 8 – Methods used to quantify turbulence in the publications reviewed. Particle*
 932 *tracking: refers to particle tracking velocimetry, DPIV and PLIF. Doppler velocimetry: refers*
 933 *to ADV and LDV. Other: refers to dye dispersion and bioluminescence.*

934

935 **Particle tracking velocimetry**

936 As a precursor to digital image analysis techniques, early particle imaging was carried

937 out using video recorders attached to microscopes (e.g. Saiz and Alcaraz (1992)). This

938 technique involves the direct imaging of individual tracer particles (e.g., reflective spheres or

939 phytoplankton cells) highlighted by a sheet of laser light. An image is taken and compared to

940 another image taken some small time period later. The subsequent direct image comparison

941 allows for local particle displacement to be determined. By accounting for the time delay and

942 image magnification, it is possible to map the velocity field of a tank. While this analysis has

943 proven to be computationally expensive, it does result in a high vector density with good

944 accuracy and spatial resolution (Webster et al., 2001). The image field is then divided into a

945 grid, the instantaneous velocities are decomposed into horizontal and vertical components, the

946 spatial means within a grid cell are computed. This spatial mean is then subtracted from the

947 instantaneous velocity field to yield the fluctuating component of the particle velocities,

948 which is representative of the turbulence in the flow, and, from this, the turbulent dissipation
949 rate can be determined (Marrasé et al., 1990; Saiz and Alcaraz, 1992).

950 Technological advances in velocimetry are now permitting fluid dynamicists to
951 measure the flow fields across illuminated planes within a cosm. As water is a transparent
952 medium, these techniques typically involve the illumination of particles suspended in the
953 fluid, as suspended sediment, planktonic organisms or artificially introduced reflective
954 particles. These particle tracking velocimetry techniques typically involve an external source
955 of illumination (e.g., a light or laser) and an external camera. Thus, a benefit of these
956 techniques is that they do not require apparatus to be placed in the test tank; hence, they can
957 be used with a variety of turbulence-generation methods. While advances in particle tracking
958 velocimetry now permit detailed imaging of 3D flows (Hoyer et al., 2005; Raffel et al., 2018),
959 this has yet to be applied to any bio-turbulence studies which, to date, have not progressed
960 beyond two-dimensional (2D) imaging. This technique is sometimes referred to as digital
961 particle tracking velocimetry (DPTV) (Webster et al. (2001).

962

963 **Digital Particle Imaging Velocimetry**

964 Digital particle imaging velocimetry (Digital PIV or DPIV) involves seeding the test
965 fluid with highly reflective neutrally buoyant particles. The size of the particles required is
966 dependent on the size of the fluid structures required by the study. A laser light sheet is then
967 projected into the tank resulting in an illuminated plane. This laser is synchronised to a digital
968 camera positioned perpendicular to the illuminated plane which photographs the particle
969 movement; this allows a velocity map of fluid motion to be produced. It is important to select
970 a suitable laser pulse and shutter speed to prevent signal distortion and other artefacts (Zirbel
971 et al., 2000). Older DPIV systems required the simultaneous use of two digital camera and
972 corresponding laser sheets to image 3D flow; this required unimpeded access to different

973 sides of the cosm (Eder et al., 2001). Fortunately, more modern techniques (e.g., tomographic
974 PIV; tomo-PIV) have streamlined the measurement of 3D and time-resolved (four-
975 dimensional) flows with both overall precision and higher spatial resolution (Scarano, 2012;
976 Raffel et al., 2018). Calculation of ε using PIV can be a mathematically complex procedure.
977 Assuming the turbulence is both isotropic and homogeneous, Xu and Chen (2013) simplify
978 the estimation of ε :

$$979 \quad \varepsilon = 15\nu \left\langle \left(\frac{\partial u'}{\partial x} \right)^2 \right\rangle \quad (1)$$

980 where $\langle \cdot \rangle$ denotes a mean average, ν = kinematic viscosity (m²/s), and u' = velocity
981 fluctuations in the x direction with $u' \equiv u - \langle u \rangle$ and u being the x-component velocity (m/s).

982 The introduction of lights and lasers into the fluid medium does have the potential to
983 influence the behaviour of the test organisms. Phototaxic phytoplankton species that use light
984 to orientate their swimming direction could be drawn towards the laser light. Furthermore,
985 high-intensity lasers could in theory cause photo-inhibition in photosynthetic organisms and
986 reduce the rate of primary production. Motile phototactic species could also be influenced;
987 however, Linares (2015) observed in a turbulence experiment designed to specifically study
988 the potential for laser-induced photoinhibition, that “laser exposure has little effect on
989 phytoplankton”.

990 While it is standard practice to add tracer particles to the test medium to increase the
991 SNR (Estrada et al., 1987; Fraisse et al., 2015), it is important to select an appropriate tracer.
992 The motion of any tracer is assumed to follow the flow dynamics of a setup; the extent to
993 which the tracer particles accurately follow the flow can be determined via the Stokes
994 number. The test tracer should have a Stokes number $\ll 1$ in order for the tracers to mirror
995 the fluid movement; a Stokes number < 0.1 will ensure an accuracy of 99% (Tropea and
996 Yarin, 2007). A tracer should also be neutrally buoyant and sized appropriately; a smaller

997 diameter is preferable but should be large enough to be recorded. The tracer selected should
998 be reflective so as to scatter the incident laser light; Webster et al. (2001) reported titanium
999 dioxide particles have a superior reflectance to comparably sized nylon bead tracers or kaolin.
1000 Organic substances such as *Lycopodium* pollen grains (Saiz and Kiørboe, 1995) and rheostatic
1001 fluid (made from fish scales (Latz et al., 1994; Hondzo et al., 1997) can also be used as
1002 tracers, though the addition of extra organic matter and its subsequent decomposition could
1003 influence growth rates. As such, tracers are normally added to cosms absent of test organisms.
1004 If a tracer is added to a tank containing organisms, it should be both non-toxic and non-
1005 influential on growth rates. For environmental reasons, it is prudent to avoid the use of
1006 microplastics; if the chosen tracer is a plastic, the particles should be recovered before
1007 disposal.

1008

1009 **Planar Laser Induced Fluorescence**

1010 PLIF is similar to DPIV but makes specific use of the fluorescent properties of
1011 phytoplankton. As with DPIV, a laser sheet is introduced into the fluid medium to illuminate
1012 a 2D cross-section with the cosm. Phytoplankton cells are seen to have inherent fluorescent
1013 properties due to the presence of chlorophyll compounds and other photosynthetic cellular
1014 organelles. As such, phytoplankton cells are known to exhibit a peak absorption wavelength
1015 of light at ~440 nm. Following absorption, the light is subsequently re-emitted as a lower
1016 energy photon at ~685 nm manifesting itself as fluorescence (Leeuw et al., 2013). It is
1017 possible to calibrate this fluorescence intensity to attain cell concentration as well as directly
1018 measure the velocities of individual cells akin to DPIV (Liu et al., 2017). Interestingly, as
1019 technology has progressed the robustness of PLIF systems has increased to the point where
1020 these systems can be deployed directly in the field, allowing researchers to obtain in situ
1021 measurements on fluorescent particle distributions (Franks and Jaffe, 2008). As an extension

1022 of PLIF, 3D laser induced fluorescence (3D LIF) technology exists that is able to reconstruct
1023 a 3D frozen-field image of a fluid flow by scanning perpendicular to the 2D laser sheet
1024 (Crimaldi, 2008); to date, no evidence could be found of it being applied to bio-turbulence
1025 studies. Despite the differences in technology, quantification of turbulence based on DPIV
1026 and PLIF draws upon the same calculations.

1027 Relying on fluorescence does mean that any other photo-active particles and/or
1028 chemicals in the fluid medium will obscure the fluorescent signature. In particular, the
1029 presence of CDOM can preferentially absorb certain light wavelengths and attenuate light
1030 transmission through the water. The fluorescence intensity from certain dyes are also
1031 dependent on the pH and temperature of the water (Crimaldi, 2008), so this should be
1032 corrected for to allow comparisons between studies. Also of note is the process of
1033 photobleaching by which the fluorescent intensity of a dye or phytoplankton cell diminishes
1034 over time with prolonged exposure to high-intensity light of certain wavelengths; selection of
1035 a suitable dye should prohibit these effects but dyes that are less susceptible to photobleaching
1036 are typically more costly (Crimaldi, 2008).

1037

1038 **Doppler velocimetry**

1039 Doppler velocimetry involves introducing a soundwave or laser of known frequency
1040 into a fluid medium. This beam is then reflected off moving particles within the fluid causing
1041 a measurable frequency shift. Doppler velocimetry allows the user to accurately measure 3D
1042 mm-scale velocities within a water body.

1043

1044 *Acoustic Doppler Velocimetry*

1045 Single-point velocity Acoustic Doppler Velocimeters (ADV) can be used to good
1046 effect to measure 3D point velocities. As the name would suggest, ADVs utilise the Doppler

1047 effect by which a pulse of sound of a known frequency is sent into the water from a central
1048 transducer. This pulse is reflected by particles in the water back to three receivers which
1049 calculate the motion of the water from the shifted frequency. The reflective particles in the
1050 water can be natural (e.g., sediment, microorganisms) or artificial (e.g., seeded particles in test
1051 tanks). The addition of such particles greatly improves the SNR, which is especially useful in
1052 quiescent flows.

1053 While the resolution of the instrument varies with manufacturer (as well as sampling
1054 rate and sampling volume), one can directly quantify different turbulence parameters with
1055 suitable processing by measuring Reynolds stresses (Lohrmann et al., 1995) or by fitting the
1056 Kolmogorov $-5/3$ slope to the inertial subrange of the velocity spectra (Bluteau et al., 2011).
1057 ADVs have many logistical advantages; namely, they provide a relatively simple and
1058 inexpensive way to quantify turbulence (Bluteau et al., 2011) while also being portable and
1059 robust. Furthermore, they do not require frequent calibration and are not constrained by
1060 turbidity as optical sensors are (Lohrmann et al., 1995). As well as bio-turbulence studies,
1061 ADVs are commonly used as velocity sensors in physical limnological and oceanographic
1062 studies both in the laboratory and in the field.

1063 Building upon a previous study that overlooked the quantification of turbulence
1064 (Berdalet, 1992), Berdalet et al. (2007) used a side-mounted Nortek 3D 10 MHz ADV to
1065 record current velocities at different points within a test flask placed on a shaker table.
1066 Interestingly, the ADV was mounted on the shaker table so was stationary relative to the
1067 flask. Sullivan and Swift (2003) used a Sontek ADV to quantify ϵ at different positions across
1068 a range of turbulent intensities. As with DPIV, the test medium was also seeded with
1069 microparticles in order to increase the acoustic backscatter and thus improve the SNR.
1070 Sullivan and Swift (2003) used two different mathematical techniques to calculate turbulence
1071 from the velocity measurements, providing a comparison of values which showed that the two

1072 methods yielded similar results. These researchers went to lengths to ensure that the levels of
1073 turbulence generated in the experiments were analogous to those found in the ocean (namely,
1074 $\varepsilon = 10^{-8} \text{ m}^2 \cdot \text{s}^{-3}$ for the lower turbulence level and $\varepsilon = 10^{-4} \text{ m}^2 \cdot \text{s}^{-3}$ for the higher) and compared
1075 them to published ε values. A Nortek ADV was used by Guadayol et al. (2009b) to assess the
1076 differences in ε between grid- and shaker-generated turbulence. Depending on the
1077 manufacturer, the pronged head of an ADV can have a maximum diameter $\sim 10\text{cm}$ in diameter
1078 thus limiting the size and shape of vessel in which it is possible to obtain measurements. In
1079 order to record the velocity in a small grid-generated turbulence vessel, this study made use of
1080 a set of bespoke 2 L and 15 L vessels that incorporated the transducer heads into the wall of
1081 the vessel itself. The vessels were constructed from Delrin plastic to limit the internal
1082 reflection from the tank walls. A larger 2500 L mesocosm tank was constructed with a grid of
1083 mesh size 10 cm so that the ADV could be deployed through the mesh without interfering
1084 with the grid mechanism. With regards to measuring velocities in the orbital shaker vessels, a
1085 custom-made, side-looking ADV was placed in the vessel, held in place by a posable arm also
1086 attached to the shaker as per Berdalet et al. (2007). Also of interest in these studies is the
1087 sampling time requirements; a longer sampling time is needed in larger vessels to resolve
1088 larger overturns. Thus, a minimum duration of 10 minutes was used in the grid tanks and 5
1089 minutes for the shaker tables.

1090

1091 *Laser Doppler Velocimetry*

1092 Optical Laser Doppler Velocimeters (LDV) can be used in a manner similar to
1093 acoustic Doppler velocimetry. The fluid medium is seeded with reflective beads in order to
1094 increase the SNR and then the laser is used to image particle motion within the fluid.
1095 Usefully, the technology has now advanced to the point where it is now readily commercially
1096 available with an easy installation. Unlike DPIV, only a single system is need to image 3D

1097 flows (Eder et al., 2001). Due to the use of lasers and seeded water, this method has been
1098 incorrectly referred to as DPIV in some literature; however, similar considerations regarding
1099 the introduction of laser beams to water and the addition of seeded particles discussed should
1100 be applied.

1101 In situations where it is difficult to place the sensor in the tank directly (due to size or
1102 presence of other apparatus), it is possible to image the fluid motion from outside the tank if
1103 the vessel is transparent and taking into account any inherent refractive effects. Peters and
1104 Gross (1994) mitigated this lensing effect by constructing a replica test tank solely for
1105 turbulence quantification. The replica tank was built out of transparent acrylic; it was
1106 surrounded by a second, square acrylic tank which was then filled with water. The outer layer
1107 of water surrounding the test tank reduced the ratio of refractive indices, thereby reducing the
1108 effects of refraction. The test tank was seeded with rutile (a mineral of titanium oxide) spheres
1109 of 2 to 3 μm diameter and particle velocities were measured in the u and v directions via a 2-
1110 axis laser anemometer.

1111 A summary of the pros and cons associated with each method discussed in this section
1112 can be found in Table 4.

1113

1114

1115 *Table 4 - Summary table of different turbulence measurement techniques*

Technique	Pro	Con
Particle tracking velocimetry	<ul style="list-style-type: none"> • High accuracy and spatial resolution • External to tank 	<ul style="list-style-type: none"> • Redundant technology with the advent of more powerful CPUs and digital cameras
DPIV	<ul style="list-style-type: none"> • External to tank • Produces velocity fields over the full field of view of the camera 	<ul style="list-style-type: none"> • Can be difficult to set up • Equipment set-up can be very costly • Potential for introduction of microplastics into water ways • Refraction effects need to be accounted for • Requires access to the tank from at least two directions • Requires two sets of equipment to visualise flows in 3D • Complex, highly technical experimental set-up
PLIF	<ul style="list-style-type: none"> • Can map cell concentrations as well as velocities • Can be deployed in the field in situ • External to tank • Produces velocity fields over the full field of view of the camera 	<ul style="list-style-type: none"> • Can cause photobleaching in cells • Refraction effects need to be accounted for • Complex, highly technical experimental set-up
ADV	<ul style="list-style-type: none"> • Portable and robust • Can be used in turbid water • Possible to obtain multiple turbulence characteristics 	<ul style="list-style-type: none"> • Difficult to use in tanks with moving parts • Only point measurements
LDV	<ul style="list-style-type: none"> • Simple installation and use • External to tank 	<ul style="list-style-type: none"> • Refraction effects need to be accounted for • Equipment set-up can be very costly • Potential for introduction of microplastics into water ways • Only point measurements

1116

1117 **Empirical formulae**

1118 Empirically derived formulae are used in 44% of publications to quantify turbulence
 1119 (Figure 8), reflecting the high proportion of studies using Couette cylinders and shaker tables.
 1120 In circumstances where the cosm is either too small or unsuitable to use measurement
 1121 apparatus, it is possible to approximate the level of turbulent intensity using basic

1122 measurements of the experimental set-up. This may be useful for researchers that do not have
1123 access to the high-cost, specialist measurement apparatus discussed previously. It is
1124 recommended to report turbulence quantification as dissipation rates (ϵ ; m^2/s^3) to be
1125 concurrent with physical oceanographic observations in the field and thus facilitate
1126 comparison between studies. As such, Equations (3) and (5) below have been modified to
1127 output in m^2/s^3 .

1128

1129 *Shakers*

1130 Due to their small size and vessel motion, shaker experiments have typically
1131 precluded direct fluid measurement (the exception being Zirbel et al. (2000) who used PIV).
1132 As such, Peters and Marrasé (2000) were able to retrospectively estimate ϵ in a number of
1133 studies:

1134

1135
$$\epsilon = \frac{S(d \cdot f)^3}{V} \quad (2)$$

1136 where d = distance the vessel travels in one oscillation (m); f = frequency of oscillation (Hz),
1137 V = volume of fluid (m^3), and S = surface in contact with fluid (as derived from flask
1138 geometry; m^2). The resultant ϵ value will be indicative of the order of magnitude of ϵ , not a
1139 direct equality due to approximation in turbulent length scales.

1140 Building upon this, Guadayol et al. (2009b) empirically formulated a relationship for ϵ
1141 based on direct velocity measurements across different frequencies of oscillation and orbit
1142 diameter:

1143

1144
$$\epsilon = 10^{(-5.03 - 1.56\phi + f(1.71 + 1.08\phi)) - 5} \quad (3)$$

1145 where ϕ = orbit diameter (cm). Note that Equation (3) only holds for orbital diameters
1146 between 1.4 - 3.0 cm and oscillation frequencies between 1.19 - 2.54 Hz.

1147

1148 *Vertical grids*

1149 With regards to turbulence generated by vertically-oscillating grids, ε can be estimated
1150 as a function of grid oscillation frequency, stroke length and cosm dimensions (Peters and
1151 Marrasé, 2000).

1152

1153
$$\varepsilon = \left(\frac{1}{T/4}\right) \int_0^{T/4} \frac{0.7 \cdot A_{grid}}{V} u(t)^3 dt \quad (4)$$

1154 where T = period of one oscillation (s), A_{grid} = solid area of the grid (m²), and $u(t)$ = vertical
1155 grid velocity (m/s), as calculated from oscillation frequency and stroke length. The 0.7
1156 coefficient is the empirically derived drag coefficient of a falling grid (Peters and Marrasé,
1157 2000). Note that this coefficient will change accordingly with different grid geometries and
1158 configurations; given the ad hoc nature of many turbulence studies, a prudent course of action
1159 would be to calculate the drag coefficient for different grid setups.

1160 Guadayol et al. (2009b) have also developed a series of empirical equations to
1161 describe the ε at different locations in a tank with a vertically oscillating grid. Equation (5)
1162 calculates ε at a location outside of the grid motion area:

1163

1164
$$\varepsilon = 2 \times 10^{-6} \cdot s^{9/2} \cdot M^{3/2} \cdot z^{-4} \cdot f^3 \quad (5)$$

1165 where s = stroke length (cm), M = mesh size (cm), and z = distance from the centre of the
1166 oscillation (cm). Equation (5) holds for stroke lengths between 2.8 - 40 cm; mesh sizes from
1167 0.9 - 10 cm; and, z-distances between 1 - 73 cm. See Guadayol et al. (2009b) for additional

1168 equations describing ε within the grid path as well as variations for constant and sinusoidal
1169 grid motion.

1170

1171 *Couette cylinders*

1172 In Couette cylinders, the rotational rate and shears can be easily converted to ε
1173 (Thomas and Gibson, 1990b):

1174

1175
$$\varepsilon = \nu \left(\frac{R \cdot D \cdot \pi}{60 \cdot G} \right)^2 \quad (6)$$

1176

1177 where ν = kinematic viscosity (m^2/s), R = rotational rate in revolutions per minute (rpm), D =
1178 the diameter of the outer cylinder (m), and G = the gap width (m). Note that the contents of
1179 the parentheses ($RD\pi/60G$) correspond to the value for strain (γ) in radians per second
1180 (rads/s).

1181

1182 **CONCLUSION**

1183 We have observed that experiments involving phytoplankton-turbulence interactions
1184 take many forms often dictated by budget, access to facilities and/or the background
1185 experience of the researchers themselves. This paper aimed to review the various techniques
1186 used to both generate turbulence and quantify the turbulence produced.

1187 With regards to the method of turbulence generation, most (31%) previous cosm work
1188 has been carried out using oscillating grids (as compared to aeration, Couette cylinders and
1189 shaker tables); it is our recommendation that future studies continue to make use of this
1190 method due to operational advantages and a robust set of literature and historical data for
1191 results comparison. Oscillating grids are simple, effective, and inexpensive, with 29 out of 32

1192 studies reviewed quantifying the turbulence produced. The grids themselves can generate
1193 near-isotropic turbulence across a wide range of scales. A grid setup is relatively low-cost to
1194 implement or retrofit to existing facilities using basic variable-speed motors. Furthermore,
1195 grid setups can easily be applied to large tanks ($>1\text{m}^3$) to enable capturing a wider range of
1196 turbulence length scales. It is important that a mesh barrier (e.g., MacKenzie and Kiørboe
1197 (1995) be placed between the grid area and the organism to not only reduce the risk of
1198 mechanical damage but also to create a refuge region that allows the organisms respite from
1199 the turbulence. Similarly, it is important the grids are programmed accordingly to oscillate at
1200 a frequency that provides further temporal respite from maximum turbulence. Similarly, the
1201 cosm itself and the stroke-length over which the grid should oscillate should be on the order
1202 of at least one metre to properly reflect the natural length scales of vertical overturns.

1203 With regards to our recommendation for quantification methods, Acoustic Doppler
1204 velocimeters (ADV) are both the most commonly used as well as the least complex and
1205 inexpensive of the methodologies. However, we do recognise that using an ADV within an
1206 environment with an oscillating grid does provide some logistical challenges to overcome.

1207 Phytoplankton-turbulence interactions are complex (Figure 1); however, studies of this
1208 nature are a critical tool for helping us to better understand not only how the aquatic
1209 environment functions but also how it will respond as climate change continues to alter
1210 turbulent regimes across the planet (Hallegraeff, 2010; Hinder et al., 2012). Worryingly, the
1211 number of publications of this nature has been declining in recent years (Figure 6). Only by 1)
1212 standardising future phytoplankton-turbulence experiments and 2) promoting more
1213 interdisciplinary collaboration between fluid dynamicists and aquatic ecologists will we be
1214 able to better understand the subtle, yet dominant and complex, ways that turbulence
1215 influences the microscopic lives of phytoplankton.

REFERENCES

- Aguilera, J., C. Jiménez, J. M. Rodríguez-Maroto & F. X. Niell, 1994. Influence of subsidiary energy on growth of *Dunaliella viridis* Teodoresco: the role of extra energy in algal growth. *Journal of Applied Phycology* 6(3):323-330.
- Alcaraz, M., E. Saiz, C. Marrasé & D. Vaqué, 1988. Effects of turbulence on the development of phytoplankton biomass and copepod populations in marine microcosms. *Marine Ecology Progress Series* 49:117 - 125.
- Alexander, A. C., E. Luiker, M. Finley & J. M. Culp, 2016. Chapter 8 - Mesocosm and Field Toxicity Testing in the Marine Context. In Blasco, J., P. M. Chapman, O. Campana & M. Hampel (eds) *Marine Ecotoxicology*. Academic Press, 239-256.
- Allredge, A. L., T. C. Granata, C. C. Gotschalk & T. D. Dickey, 1990. The physical strength of marine snow and its implications for particle disaggregation in the ocean. *Limnology and Oceanography* 35(7):1415-1428.
- Arin, L., C. Marrasé, M. Maar, F. Peters, M. M. Sala & M. Alcaraz, 2002. Combined effects of nutrients and small-scale turbulence in a microcosm experiment. I. Dynamics and size distribution of osmotrophic plankton. *Aquatic Microbial Ecology* 29(1):51-61.
- Bakus, G., J., 1973. Some effects of turbulence and light on competition between two species of phytoplankton. *Investigación Pesquera* 37:87-100.
- Båmstedt, U. & H. Larsson, 2018. An indoor pelagic mesocosm facility to simulate multiple water-column characteristics. *International Aquatic Research* 10(1):13-29.
- Banse, K., 1991. Rates of phytoplankton cell division in the field and in iron enrichment experiments. *Limnology and Oceanography* 36(8):1886-1898.

- Beauvais, S., M. L. Pedrotti, J. Egge, K. Iversen & C. Marrasé, 2006. Effects of turbulence on TEP dynamics under contrasting nutrient conditions: Implications for aggregation and sedimentation processes. *Marine Ecology Progress Series* 323:47-57.
- Behm, J. E., B. R. Waite, S. T. Hsieh & M. R. Helmus, 2018. Benefits and limitations of three-dimensional printing technology for ecological research. *BioMed Central Ecology* 18(1):32-32.
- Berdalet, E., 1992. Effects of turbulence on the marine dinoflagellate *Gymnodinium nelsonii*. *Journal of Phycology* 28(3):267-272.
- Berdalet, E. & M. Estrada, 1993. Effects of turbulence on several phytoplankton species. In Smayda, T. J. & Y. Shimizu (eds) *Toxic Phytoplankton Blooms in the Sea. Developments in Marine Biology*, vol 3. Elsevier, Amsterdam, The Netherlands, 737 - 740.
- Berdalet, E., F. Peters, V. L. Koumandou, C. Roldán, Ò. Guadayol & M. Estrada, 2007. Species-specific physiological response of dinoflagellates to quantified small-scale turbulence. *Journal of Phycology* 43(5):965-977.
- Bergkvist, J., I. Klawonn, M. J. Whitehouse, G. Lavik, V. Brüchert & H. Ploug, 2018. Turbulence simultaneously stimulates small- and large-scale CO₂ sequestration by chain-forming diatoms in the sea. *Nature Communications* 9(1).
- Bienfang, P. K., P. J. Harrison & L. M. Quarmby, 1982. Sinking rate response to depletion of nitrate, phosphate and silicate in four marine diatoms. *Marine Biology* 67(3):295-302.
- Bluteau, C. E., N. L. Jones & G. N. Ivey, 2011. Estimating turbulent kinetic energy dissipation using the inertial subrange method in environmental flows. *Limnology and Oceanography: Methods* 9(7):302-321.
- Chen, D., K. Muda, K. Jones, J. Leftly & P. Stansby, 1998. Effect of shear on growth and motility of *Alexandrium minutum* Halim, a red-tide dinoflagellate. In Reguera, B., J. Blanco, M. L. Fernández & T. Wyatt (eds) *Harmful algae. Xunta de Galicia and Intergovernmental Oceanographic Commission of UNESCO, Vigo, Galicia, Spain*, 352-355.

- Coble, P. G., 2007. Marine Optical Biogeochemistry: The Chemistry of Ocean Color. *Chemical Reviews* 107(2):402-418.
- Couette, M., 1890. Distinction de deux régimes dans le mouvement des fluides. *Journal de Physique Théorique et Appliquée* 9(1):414-424.
- Cózar, A. & F. Echevarría, 2005. Size structure of the planktonic community in microcosms with different levels of turbulence. *Scientia Marina* 69(2):187-197.
- Crimaldi, J. P., 2008. Planar laser induced fluorescence in aqueous flows. *Experiments in Fluids* 44(6):851-863.
- Crossland, N. O. & T. W. La Point, 1992. The design of mesocosm experiments. *Environmental Toxicology and Chemistry* 11(1):1-4.
- Davis, E. A., J. Dedrick, C. S. French, H. W. Milner, J. Myers, J. H. C. Smith & H. A. Spoehr, 1953. Laboratory experiments on *Chlorella* culture at the Carnegie Institution of Washington department of plant biology. In Burlew, J. S. (ed) *Algal Culture from Laboratory to Pilot Plant*. 5th edn. Carnegie Institution of Washington, Washington DC, 105-153.
- Dawidowicz, P., 1990. The effect of *Daphnia* on filament length of blue-green algae. *Hydrobiologia* 191(1):265-268.
- Delaney, M. P., 2003. Effects of temperature and turbulence on the predator-prey interactions between a heterotrophic flagellate and a marine bacterium. *Microbial ecology* 45(3):218-225.
- Dempsey, H. P., 1982. The effects of turbulence on three algae: *Skeletonema costatum*, *Gonyaulax tamarensis*, *Heterocapsa triquetra*. Massachusetts Institute of Technology.
- Dolan, J. R., N. Sall, A. Metcalfe & B. Gasser, 2003. Effects of turbulence on the feeding and growth of a marine oligotrich ciliate. *Aquatic Microbial Ecology* 31(2):183-192.

- Donaghay, P. L. & E. Klos, 1985. Physical, chemical and biological responses to simulated wind and tidal mixing in experimental marine ecosystems. *Marine Ecology Progress Series* 26(1/2):35-45.
- Eder, A., B. Durst & M. Jordan, 2001. Laser-Doppler Velocimetry — Principle and Application to Turbulence Measurements. In Mayinger, F. & O. Feldmann (eds) *Optical Measurements: Techniques and Applications*. Springer, Berlin, Heidelberg, 117-138.
- Eppley, R. W., P. Koeller & G. T. Wallace, 1978. Stirring influences the phytoplankton species composition within enclosed columns of coastal sea water. *Journal of Experimental Marine Biology and Ecology* 32(3):219-239.
- Escaravage, V., L. P. M. J. Wetsteyn, T. C. Prins, A. J. Pouwer, A. de Kruyff, M. Vink-Lievaart, C. M. van der Voom, J. C. H. Peeters & A. C. Smaal, 1997. The impact of marine eutrophication on phytoplankton, zooplankton and benthic suspension feeders. Stratification in mesocosms, a pilot experiment. Ministerie van Verkeer en Waterstaat, The Netherlands, 52.
- Estrada, M., M. Alcaraz & C. Marrasé, 1987. Effects of turbulence on the composition of phytoplankton assemblages in marine microcosms. *Marine Ecology Progress Series* 38:267-281.
- Fogg, G. E. & Than-Tun, 1960. Interrelations of photosynthesis and assimilation of elementary nitrogen in a blue-green alga. *Proceedings of the Royal Society of London Series B Biological Sciences* 153(950):111-127.
- Fraisse, S., M. Bormans & Y. Lagadeuc, 2015. Turbulence effects on phytoplankton morphofunctional traits selection. *Limnology and Oceanography* 60(3):872-884.
- Franks, P. J. S., 2001. Turbulence avoidance: An alternate explanation of turbulence-enhanced ingestion rates in the field. *Limnology and Oceanography* 46(4):959-963.
- Franks, P. J. S. & J. S. Jaffe, 2008. Microscale variability in the distributions of large fluorescent particles observed in situ with a planar laser imaging fluorometer. *Journal of Marine Systems* 69(3):254-270.

- Fuchs, H. L. & G. P. Gerbi, 2016. Seascape-level variation in turbulence- and wave-generated hydrodynamic signals experienced by plankton. *Progress in Oceanography* 141:109-129.
- Garrison, H. S. & K. W. Tang, 2014. Effects of episodic turbulence on diatom mortality and physiology, with a protocol for the use of Evans Blue stain for live–dead determinations. *Hydrobiologia* 738(1):155-170.
- Gibson, C. H. & W. H. Thomas, 1995. Effects of turbulence intermittency on growth inhibition of a red tide dinoflagellate, *Gonyaulax polyedra* Stein. *Journal of Geophysical Research: Oceans* 100(C12):24841-24846.
- Gonzalez-Fernandez, C., J. Toullec, C. Lambert, N. Le Goic, M. Seoane, B. Moriceau, A. Huvet, M. Berchel, D. Vincent, L. Courcot, P. Soudant & I. Paul-Pont, 2019. Do transparent exopolymeric particles (TEP) affect the toxicity of nanoplastics on *Chaetoceros neogracile*? *Environmental Pollution* 250:873-882.
- Grobbelaar, J. U., 1989. Do light/dark cycles of medium frequency enhance phytoplankton productivity? *Journal of Applied Phycology* 1(4):333-340.
- Guadayol, O., C. Marrasé, F. Peters, E. Berdalet, N. Roldá & A. Sabata, 2009a. Responses of coastal osmotrophic planktonic communities to simulated events of turbulence and nutrient load throughout a year. *Journal of Plankton Research* 31(6):583-600.
- Guadayol, Ò., F. Peters, J. E. Stiansen, C. Marrasé & A. Lohrmann, 2009b. Evaluation of oscillating grids and orbital shakers as means to generate isotropic and homogeneous small-scale turbulence in laboratory enclosures commonly used in plankton studies. *Limnology and Oceanography: Methods* 7(APR.):287-303.
- Guasto, J. S., R. Rusconi & R. Stocker, 2012. Fluid mechanics of planktonic microorganisms. *Annual Review of Fluid Mechanics* 44:373 - 400.
- Hallegraeff, G. M., 2010. Ocean climate change, phytoplankton community responses, and harmful algal blooms: a formidable predictive challenge. *Journal of Phycology* 46(2):220-235.

- Havskum, H., 2003. Effects of small-scale turbulence on interactions between the heterotrophic dinoflagellate *Oxyrrhis marina* and its prey, *Isochrysis* sp. *Ophelia* 57(3):125-135.
- Havskum, H. & P. J. Hansen, 2006. Net growth of the bloom-forming dinoflagellate *Heterocapsa triquetra* and pH: Why turbulence matters. *Aquatic Microbial Ecology* 42(1):55-62.
- Havskum, H., P. J. Hansen & E. Berdalet, 2005. Effect of turbulence on sedimentation and net population growth of the dinoflagellate *Ceratium tripos* and interactions with its predator, *Fragilidium subglobosum*. *Limnology and Oceanography* 50(5):1543-1551.
- Hellung-Larsen, P. & I. Lyhne, 1992. Effect of shaking on the growth of diluted cultures of *Tetrahymena*. *The Journal of Protozoology* 39(2):345-349.
- Hinder, S. L., G. C. Hays, M. Edwards, E. C. Roberts, A. W. Walne & M. B. Gravenor, 2012. Changes in marine dinoflagellate and diatom abundance under climate change. *Nature Climate Change* 2(4):271-275.
- Hondzo, M. M., A. Kapur & C. A. Lembi, 1997. The effect of small-scale fluid motion on the green alga *Scenedesmus quadricauda*. *Hydrobiologia* 364(2):225-235.
- Howarth, R. W., T. Butler, K. Lunde, D. Swaney & C. R. Chu, 1993. Turbulence and planktonic nitrogen fixation: a mesocosm experiment. *Limnology and Oceanography* 38(8):1696-1711.
- Hoyer, K., M. Holzner, B. Lüthi, M. Guala, A. Liberzon & W. Kinzelbach, 2005. 3D scanning particle tracking velocimetry. *Experiments in Fluids* 39(5):923.
- Huisman, J., P. Van Oostveen & F. J. Weissing, 1999. Critical depth and critical turbulence: Two different mechanisms for the development of phytoplankton blooms. *Limnology and Oceanography* 44(7):1781-1787.
- Iversen, K. R., R. Primicerio, A. Larsen, J. K. Egge, F. Peters, Ó. Guadayol, A. Jacobsen, H. Havskum & C. Marrasé, 2009. Effects of small-scale turbulence on lower trophic levels under different nutrient conditions. *Journal of Plankton Research* 32(2):197-208.

- Juhl, A. R. & M. I. Latz, 2002. Mechanisms of fluid shear-induced inhibition of population growth in a red-tide dinoflagellate. *Journal of Phycology* 38(4):683-694.
- Juhl, A. R., V. L. Trainer & M. I. Latz, 2001. Effect of fluid shear and irradiance on population growth and cellular toxin content of the dinoflagellate *Alexandrium fundyense*. *Limnology and Oceanography* 46(4):758-764.
- Juhl, A. R., V. Velazquez & M. I. Latz, 2000. Effect of growth conditions on flow-induced inhibition of population growth of a red-tide dinoflagellate. *Limnology and Oceanography* 45(4):905-915.
- Kaku, V. J., M. C. Boufadel & A. D. Venosa, 2006. Evaluation of mixing energy in laboratory flasks used for dispersant effectiveness testing. *Journal of Environmental Engineering* 132(1):93-101.
- Kangas, P. C. & W. H. Adey, 2008. Mesocosm Management. In Jørgensen, S. E. & B. D. Fath (eds) *Encyclopedia of Ecology*. Academic Press, Oxford, 2308-2313.
- Karp-Boss, L., E. Boss & P. A. Jumars, 2000. Motion of dinoflagellates in a simple shear flow. *Limnology and Oceanography* 45(7):1594-1602.
- Karp-Boss, L. & P. A. Jumars, 1998. Motion of diatom chains in steady shear flow. *Limnology and Oceanography* 43(8):1767-1773.
- Katija, K., 2012. Biogenic inputs to ocean mixing. *The Journal of Experimental Biology* 215(6):1040-1049.
- Kilham, P., 1971. A hypothesis concerning silica and the freshwater planktonic diatoms. *Limnology and Oceanography* 16(1):10-18.
- Kjørboe, T., 1993. Turbulence, phytoplankton cell size, and the structure of pelagic food webs. *Advances in Marine Biology* 29:1-72.
- Kjørboe, T., K. P. Andersen & H. G. Dam, 1990. Coagulation efficiency and aggregate formation in marine phytoplankton. *Marine Biology* 107(2):235-245.
- Kirke, B. K., Pumping downwards to prevent algal blooms. In: IWA 2nd World Water Congress, Berlin, 2001.

- Köhler, J., 1997. Measurement of in situ growth rates of phytoplankton under conditions of simulated turbulence. *Journal of Plankton Research* 19(7):849-862.
- Kromkamp, J., F. Schanz, M. Rijkeboer, E. Berdalet, B. Kim & H. J. Gons, 1992. Influence of the mixing regime on algal photosynthetic performance in laboratory scale enclosures. *Hydrobiologia* 238(1):111-118.
- Latz, M. I., J. Allen, S. Sarkar & J. Rohr, 2009. Effect of fully characterized unsteady flow on population growth of the dinoflagellate *Lingulodinium polyedrum*. *Limnology and Oceanography* 54(4):1243-1256.
- Latz, M. I., J. F. Case & R. L. Gran, 1994. Excitation of bioluminescence by laminar fluid shear associated with simple Couette flow. *Limnology and Oceanography* 39(6):1424-1439.
- Latz, M. I., J. C. Nauen & J. Rohr, 2004. Bioluminescence response of four species of dinoflagellates to fully developed pipe flow. *Journal of Plankton Research* 26(12):1529-1546.
- Latz, M. I. & J. Rohr, 1999. Luminescent response of the red tide dinoflagellate *Lingulodinium polyedrum* to laminar and turbulent flow. *Limnology and Oceanography* 44(6):1423-1435.
- Laws, E. A., K. L. Terry, J. Wickman & M. S. Chalup, 1983. A simple algal production system designed to utilize the flashing light effect. *Biotechnology and Bioengineering* 25(10):2319-2335.
- Lazier, J. R. N. & K. H. Mann, 1989. Turbulence and the diffusive layers around small organisms. *Deep Sea Research Part A Oceanographic Research Papers* 36(11):1721-1733.
- Leeuw, T., E. S. Boss & D. L. Wright, 2013. In situ measurements of phytoplankton fluorescence using low cost electronics. *Sensors* 13(6):7872-7883.
- Leterme, S. C., I. Kesaulya, J. G. Mitchell & L. Seuront, 2008. The impact of turbulence and phytoplankton dynamics on foam formation, seawater viscosity and chlorophyll concentrations in the eastern English Channel. *Oceanologia* 50(2):167-182.

- Linares, M. C., 2015. Effects of turbulence and laser exposure on phytoplankton behavior. Universitat Politècnica de Catalunya.
- Liu, F., L. Zeng, Y. H. Wu, B. Baoligao & X. Chen, 2017. Vertical distribution of motile phytoplankton in density currents. In: Li, P. (ed) 3rd International Conference on Water Resource and Environment (WRE 2017), Qingdao, China, 26–29 June 2017. IOP Conference Series: Earth and Environmental Science, vol 82. IOP Publishing, p 012073.
- Llaveria, G., E. Garcés, O. N. Ross, R. I. Figueroa, N. Sampedro & E. Berdalet, 2010. Small-scale turbulence can reduce parasite infectivity to dinoflagellates. *Marine Ecology Progress Series* 412:45-56.
- Lohrmann, A., R. Cabrera, G. Gelfenbaum & J. Haines, 1995. Direct measurements of Reynolds stress with an acoustic Doppler velocimeter. In: Anderson, S.P., G.F. Appell & A. J. Williams III (eds) Proceedings of the IEEE Fifth Working Conference on Current Measurement, St. Petersburg, FL, USA, 7-9 Feb 1995. IEEE, p 205-210.
- Long, J. D., G. W. Smalley, T. Barsby, J. T. Anderson & M. E. Hay, 2007. Chemical cues induce consumer-specific defenses in a bloom-forming marine phytoplankton. *Proceedings of the National Academy of Sciences* 104(25):10512-10517.
- Lüring, M., 1998. Effect of grazing-associated infochemicals on growth and morphological development in *Scenedesmus acutus* (Chlorophyceae). *Journal of Phycology* 34(4):578-586.
- Maar, M., L. Arin, R. Simó, M.-M. Sala, F. Peters & C. Marrasé, 2002. Combined effects of nutrients and small-scale turbulence in a microcosm experiment. II. Dynamics of organic matter and phosphorus. *Aquatic Microbial Ecology* 29(1):63-72.
- Mackenzie, B. R. & T. Kiørboe, 1995. Encounter rates and swimming behavior of pause-travel and cruise larval fish predators in calm and turbulent laboratory environments. *Limnology and Oceanography* 40(7):1278-1289.

- Margalef, R., 1997. Turbulence and marine life. In: Marrasé, C., E. Saiz & J. M. Redondo (eds) *Scientia Marina: Lectures on plankton and turbulence*. Vol 61 (SUPPL.1), 109-123.
- Marrasé, C., J. H. Costello, T. Granata & J. R. Strickler, 1990. Grazing in a turbulent environment: Energy dissipation, encounter rates, and efficacy of feeding currents in *Centropages hamatus*. *Proceedings of the National Academy of Sciences of the United States of America* 87(5):1653-1657.
- Martin, J. H. & R. Michael Gordon, 1988. Northeast Pacific iron distributions in relation to phytoplankton productivity. *Deep Sea Research Part A Oceanographic Research Papers* 35(2):177-196.
- Martínez, R. A., A. Calbet & E. Saiz, 2017. Effects of small-scale turbulence on growth and grazing of marine microzooplankton. *Aquatic Sciences* 80(1).
- Matheson, F. E., 2008. Microcosms. In Jørgensen, S. E. & B. D. Fath (eds) *Encyclopedia of Ecology*. Academic Press, Oxford, 2393-2397.
- Metcalf, A. M., T. J. Pedley & T. F. Thingstad, 2004. Incorporating turbulence into a plankton foodweb model. *Journal of Marine Systems* 49(1-4):105-122.
- Moisander, P. H., J. L. Hench, K. Kononen & H. W. Paerl, 2002. Small-scale shear effects on heterocystous cyanobacteria. *Limnology and Oceanography* 47(1):108-119.
- Musielak, M. M., L. E. E. Karp-Boss, P. A. Jumars & L. J. Fauci, 2009. Nutrient transport and acquisition by diatom chains in a moving fluid. *Journal of Fluid Mechanics* 638:401-421.
- Naselli-Flores, L., T. Zohary & J. Padisák, 2020. Life in suspension and its impact on phytoplankton morphology: an homage to Colin S. Reynolds. *Hydrobiologia* 848:7-30 (2021).
- Nedbal, L., V. Tichý, F. Xiong & J. U. Grobbelaar, 1996. Microscopic green algae and cyanobacteria in high-frequency intermittent light. *Journal of Applied Phycology* 8(4):325-333.

- Nejstgaard, J., C. , L.-J. Naustvoll & A. Sazhin, 2001a. Correcting for underestimation of microzooplankton grazing in bottle incubation experiments with mesozooplankton. *Marine Ecology Progress Series* 221:59-75.
- Nejstgaard, J., C., B. H. Hygum, L.-J. Naustvoll & U. Båmstedt, 2001b. Zooplankton growth, diet and reproductive success compared in simultaneous diatom- and flagellate-microzooplankton-dominated plankton blooms. *Marine Ecology Progress Series* 221:77-91.
- Nerheim, S., J. E. Stiansen & H. Svendsen, 2002. Grid-generated turbulence in a mesocosm experiment. *Hydrobiologia* 484:61-73.
- Odum, E. P., 1984. The Mesocosm. *BioScience* 34(9):558-562.
- Okubo, A., 1976. Remarks on the use of 'diffusion diagrams' in modeling scale-dependent diffusion. *Deep Sea Research and Oceanographic Abstracts* 23(12):1213-1214.
- Oviatt, C. A., 1981. Effects of different mixing schedules on phytoplankton, zooplankton and nutrients in marine microcosms. *Marine Ecology Progress Series* 4:57-67.
- Paczkowska, J., O. F. Rowe, L. Schlüter, C. Legrand, B. Karlson & A. Andersson, 2017. Allochthonous matter: An important factor shaping the phytoplankton community in the Baltic Sea. *Journal of Plankton Research* 39(1):23-34.
- Padisák, J., É. Soróczki-Pintér & Z. Reznér, 2003. Sinking properties of some phytoplankton shapes and the relation of form resistance to morphological diversity of plankton - an experimental study. *Hydrobiologia* 500:243-257.
- Pahlow, M., U. Riebesell & D. A. Wolf-Gladrow, 1997. Impact of cell shape and chain formation on nutrient acquisition by marine diatoms. *Limnology and Oceanography* 42(8):1660-1672.

- Pannard, A., M. Bormans, S. Lefebvre, P. Claquin & Y. Lagadeuc, 2007. Phytoplankton size distribution and community structure: influence of nutrient input and sedimentary loss. *Journal of Plankton Research* 29(7):583-598.
- Parsons, T. R., P. J. Harrison & R. Waters, 1978. An experimental simulation of changes in diatom and flagellate blooms. *Journal of Experimental Marine Biology and Ecology* 32(3):285-294.
- Pasciak, W. J. & J. Gavis, 1975. Transport limited nutrient uptake rates in *Ditylum brightwellii*. *Limnology and Oceanography* 20(4):604-617.
- Peters, F., L. Arin, C. Marrasé, E. Berdalet & M. M. Sala, 2006. Effects of small-scale turbulence on the growth of two diatoms of different size in a phosphorus-limited medium. In: Peters, F. & C. Hannah (eds) *Workshop on Future Directions in Modelling Physical-Biological Interactions (WKFDPI)*, Barcelona, Catalunya, Spain, 7-9 March 2004. *Journal of Marine Systems* 61(3-4):134-148.
- Peters, F., J. W. Choi & T. Gross, 1996. *Paraphysomonas imperforata* (Protista, Chrysomonadida) under different turbulence levels: feeding, physiology and energetics. *Marine Ecology Progress Series* 134:235-245.
- Peters, F. & T. Gross, 1994. Increased grazing rates of microplankton in response to small-scale turbulence. *Marine Ecology Progress Series* 115(3):299-308.
- Peters, F. & C. Marrasé, 2000. Effects of turbulence on plankton: An overview of experimental evidence and some theoretical considerations. *Marine Ecology Progress Series* 205:291-306.
- Peters, F., C. Marrasé, H. Havskum, F. Rassoulzadegan, J. Dolan, M. Alcaraz & J. M. Gasol, 2002. Turbulence and the microbial food web: Effects on bacterial losses to predation and on community structure. *Journal of Plankton Research* 24(4):321-331.
- Peters, F. & J. M. Redondo, 1997. Turbulence generation and measurement: Application to studies on plankton. In: Marrasé, C., E. Saiz & J. M. Redondo (eds) *Scientia Marina: Lectures on plankton and turbulence*. Vol 61 (SUPPL.1), 205-228.

- Petersen, J. E., L. P. Sanford & W. M. Kemp, 1998. Coastal plankton responses to turbulent mixing in experimental ecosystems. *Marine Ecology Progress Series* 171:23-41.
- Pollingher, U. & E. Zemel, 1981. In situ and experimental evidence of the influence of turbulence on cell division processes of *Peridinium cinctum* forma *westii* (Lemm.) Lefèvre. *British Phycological Journal* 16(3):281-287.
- Prairie, J. C., K. R. Sutherland, K. J. Nickols & A. M. Kaltenberg, 2012. Biophysical interactions in the plankton: A cross-scale review. *Limnology and Oceanography: Fluids and Environments* 2(1):121-145.
- Pringle, J. M., 2007. Turbulence avoidance and the wind-driven transport of plankton in the surface Ekman layer. *Continental Shelf Research* 27(5):670-678.
- Raffel, M., C. E. Willert, F. Scarano, C. J. Kähler, S. T. Wereley & J. Kompenhans, 2018. Particle image velocimetry: a practical guide. Springer.
- Regel, R. H., J. D. Brookes, G. G. Ganf & R. W. Griffiths, 2004. The influence of experimentally generated turbulence on the Mash01 unicellular *Microcystis aeruginosa* strain. *Hydrobiologia* 517(1):107-120.
- Reynolds, C. S., 2009. Biological–Physical Interactions. In Likens, G. E. (ed) *Encyclopedia of Inland Waters*. Academic Press, Oxford, 515-521.
- Richmond, A. & A. Vonshak, 1978. Spirulina culture in Israel. *Archiv für Hydrobiologie - Beihefte Ergebnisse der Limnologie* 11:274 - 280.
- Rijkeboer, M., F. de Bles & H. J. Gons, 1990. Laboratory scale enclosure: concept, construction and operation. *Journal of Plankton Research* 12(1):231-244.
- Rohr, J., J. Allen, J. Losee & M. I. Latz, 1997. The use of bioluminescence as a flow diagnostic. *Physics Letters A* 228(6):408-416.

- Rohr, J., M. Hyman, S. Fallon & M. I. Latz, 2002. Bioluminescence flow visualization in the ocean: an initial strategy based on laboratory experiments. *Deep Sea Research Part I: Oceanographic Research Papers* 49(11):2009-2033.
- Rohr, J., J. Losee & J. Hoyt, 1990. Stimulation of bioluminescence by turbulent pipe flow. *Deep Sea Research Part A, Oceanographic Research Papers* 37(10):1639-1646.
- Ross, O. N. & J. Sharples, 2007. Phytoplankton motility and the competition for nutrients in the thermocline. *Marine Ecology Progress Series* 347:21-38.
- Ross, O. N. & J. Sharples, 2008. Swimming for survival : A role of phytoplankton motility in a stratified turbulent environment. *Journal of Marine Systems* 70(3-4):248-262.
- Rothschild, B. J. & T. R. Osborn, 1988. Small-scale turbulence and plankton contact rates. *Journal of Plankton Research* 10(3):465-474.
- Saiz, E. & M. Alcaraz, 1992. Free-swimming behaviour of *Acartia clausi* (Copepoda: Calanoida) under turbulent water movement. *Marine Ecology Progress Series* 80(2-3):229-236.
- Saiz, E. & T. Kiørboe, 1995. Predatory and suspension feeding of the copepod *Acartia tonsa* in turbulent environments. *Oceanographic Literature Review* 43(1):59.
- Sanford, L. P., 1997. Turbulent mixing in experimental ecosystem studies. *Marine Ecology Progress Series* 161:265-293.
- Santschi, P. H., 1985. The MERL mesocosm approach for studying sediment-water interactions and ecotoxicology. *Environmental Technology Letters* 6(1-11):335-350.
- Sato, T., D. Yamada & S. Hirabayashi, 2010. Development of virtual photobioreactor for microalgae culture considering turbulent flow and flashing light effect. *Energy Conversion and Management* 51(6):1196-1201.

- Savidge, G., 1981. Studies of the effects of small-scale turbulence on phytoplankton. *Journal of the Marine Biological Association of the United Kingdom* 61(2):477-488.
- Scarano, F., 2012. Tomographic PIV: principles and practice. *Measurement Science and Technology* 24(1):012001.
- Schapira, M., L. Seuront & V. Gentilhomme, 2006. Effects of small-scale turbulence on *Phaeocystis globosa* (Prymnesiophyceae) growth and life cycle. *Journal of Experimental Marine Biology and Ecology* 335(1):27-38.
- Schöne, H., 1970. Untersuchungen zur ökologischen Bedeutung des Seegangs für das Plankton mit besonderer Berücksichtigung mariner Kieselalgen. *Internationale Revue der gesamten Hydrobiologie und Hydrographie* 55(4):595-677.
- Schwartz, E. R., R. X. Poulin, N. Mojib & J. Kubanek, 2016. Chemical ecology of marine plankton. *Natural Product Reports* 33(7):843-860.
- Sengupta, A., F. Carrara & R. Stocker, 2017. Phytoplankton can actively diversify their migration strategy in response to turbulent cues. *Nature* 543:555-558.
- Simoncelli, S., S. J. Thackeray & D. J. Wain, 2019. Effect of temperature on zooplankton vertical migration velocity. *Hydrobiologia* 829(1):143-166.
- Smayda, T. J. & C. S. Reynolds, 2001. Community assembly in marine phytoplankton: Application of recent models to harmful dinoflagellate blooms. *Journal of Plankton Research* 23(5):447-461.
- Smith, B. C. & A. Persson, 2005. Synchronization of encystment of *Scrippsiella lachrymosa* (Dinophyta). *Journal of Applied Phycology* 17(4):317-321.
- Solomon, K. R. & M. Hanson, 2014. Mesocosms and Microcosms (Aquatic) *Encyclopedia of Toxicology: Third Edition*. 223-226.

- Sonntag, N. C. & T. R. Parsons, 1979. Mixing an enclosed, 1300m³ water column: effects on the planktonic food web. *Journal of Plankton Research* 1(1):85-102.
- Staehr, P. A. & K. Sand-Jensen, 2006. Seasonal changes in temperature and nutrient control of photosynthesis, respiration and growth of natural phytoplankton communities. *Freshwater Biology* 51(2):249-262.
- Steele, J. H., D. M. Farmer & E. W. Henderson, 1977. Circulation and temperature structure in large marine enclosures. *Journal of the Fisheries Research Board of Canada* 34(8):1095-1104.
- Stoecker, D. K., A. Long, S. E. Suttles & L. P. Sanford, 2006. Effect of small-scale shear on grazing and growth of the dinoflagellate *Pfiesteria piscicida*. *Harmful Algae* 5(4):407-418.
- Stokes, M. D., G. B. Deane, M. I. Latz & J. Rohr, 2004. Bioluminescence imaging of wave-induced turbulence. *Journal of Geophysical Research: Oceans* 109(C1):1-8.
- Striebel, M., L. Kirchmaier & P. Hingsamer, 2013. Different mixing techniques in experimental mesocosms—does mixing affect plankton biomass and community composition? *Limnology and Oceanography: Methods* 11(4):176-186.
- Sullivan, J. M. & E. Swift, 2003. The effect of small-scale turbulence on net growth rate and size of ten species of marine dinoflagellates. *Journal of Phycology* 39:83-94.
- Sullivan, J. M., E. Swift, P. L. Donaghay & J. E. B. Rines, 2003. Small-scale turbulence affects the division rate and morphology of two red-tide dinoflagellates. *Harmful Algae* 2(3):183-199.
- Svensen, C., J. K. Egge & J. E. Stiansen, 2001. Can silicate and turbulence regulate the vertical flux of biogenic matter? A mesocosm study. *Marine Ecology Progress Series* 217:67-80.
- Sverdrup, H. U., 1953. On conditions for the vernal blooming of phytoplankton. *ICES Journal of Marine Science* 18(3):287-295.

- Talling, J. F., 1960. Comparative laboratory and field studies of photosynthesis by a marine planktonic diatom. *Limnology and Oceanography* 5(1):62-77.
- Thomas, W. H. & C. H. Gibson, 1990a. Effects of small-scale turbulence on microalgae. *Journal of Applied Phycology* 2(1):71-77.
- Thomas, W. H. & C. H. Gibson, 1990b. Quantified small-scale turbulence inhibits a red tide dinoflagellate, *Gonyaulax polyedra* Stein. *Deep Sea Research Part A Oceanographic Research Papers* 37(10):1583-1593.
- Thomas, W. H. & C. H. Gibson, 1992. Effects of quantified small-scale turbulence on the dinoflagellate, *Gymnodium sanguineum (splendens)*: contrasts with *Gonyaulax (Lingulodinium) polyedra*, and the fishery implication. *Deep Sea Research Part A Oceanographic Research Papers* 39(7):1429-1437.
- Thomas, W. H., D. L. R. Seibert, M. Alden, A. Neori & P. Eldridge, 1984a. Yields, photosynthetic efficiencies and proximate composition of dense marine microalgal cultures. I. Introduction and *Phaeodactylum tricornutum* experiments. *Biomass* 5(3):181-209.
- Thomas, W. H., D. L. R. Seibert, M. Alden, A. Neori & P. Eldridge, 1984b. Yields, photosynthetic efficiencies and proximate composition of dense marine microalgal cultures. II. *Dunaliella primolecta* and *Tetraselmis suecica* experiments. *Biomass* 5(3):211-225.
- Thomas, W. H., D. L. R. Seibert, M. Alden, A. Neori & P. Eldridge, 1984c. Yields, photosynthetic efficiencies and proximate composition of dense marine microalgal cultures. III. *Isochrysis* sp. and *Monallantus salina* experiments and comparative conclusions. *Biomass* 5(4):299-316.
- Thomas, W. H., C. T. Tynan & C. H. Gibson, 1997. Turbulence-phytoplankton interrelationships. In Round, F. E. & D. J. Chapman (eds) *Progress in Phycological Research*. vol 12. Biopress Ltd, Bristol, UK, 283-324.
- Tropea, C. & A. L. Yarin, 2007. *Springer handbook of experimental fluid mechanics*. Springer Science & Business Media.

- Turkoglu, M., 2013. Red tides of the dinoflagellate *Noctiluca scintillans* associated with eutrophication in the Sea of Marmara (the Dardanelles, Turkey). *Oceanologia* 55(3):709-732.
- Tuttle, R. C. & A. R. Loeblich, 1975. An optimal growth medium for the dinoflagellate *Cryptothecodinium cohnii*. *Phycologia* 14(1):1-8.
- Tynan, C. T., 1993. The effects of small-scale turbulence on dinoflagellates. University of California, San Diego.
- Visser, P. M., B. W. Ibelings, M. Bormans & J. Huisman, 2016. Artificial mixing to control cyanobacterial blooms: a review. *Aquatic Ecology* 50(3):423-441.
- Waller, W. T. & H. J. Allen, 2008. Acute and Chronic Toxicity. In Jørgensen, S. E. & B. D. Fath (eds) *Encyclopedia of Ecology*. Academic Press, Oxford, 32-43.
- Walsby, A. E., 1971. Pressure relationships of gas vacuoles. *Proceedings of the Royal Society of London B* 178:301-326.
- Warnaars, T. A., M. Hondzo & M. A. Carper, 2006. A desktop apparatus for studying interactions between microorganisms and small-scale fluid motion. *Hydrobiologia* 563(1):431-443.
- Waterhouse, A. F., J. A. MacKinnon, J. D. Nash, M. H. Alford, E. Kunze, H. L. Simmons, K. L. Polzin, L. C. S. Laurent, O. M. Sun, R. Pinkel, L. D. Talley, C. B. Whalen, T. N. Huussen, G. S. Carter, I. Fer, S. Waterman, A. C. N. Garabato, T. B. Sanford & C. M. Lee, 2014. Global patterns of diapycnal mixing from measurements of the turbulent dissipation rate. *Journal of Physical Oceanography* 44(7):1854-1872.
- Webster, D. R., A. Brathwaite & J. Yen, 2004. A novel laboratory apparatus for simulating isotropic oceanic turbulence at low Reynolds number. *Limnology and Oceanography: Methods* 2(JAN.):1-12.
- Webster, D. R., P. J. W. Roberts & L. Ra'ad, 2001. Simultaneous DPTV/PLIF measurements of a turbulent jet. *Experiments in Fluids* 30(1):65-72.

- White, A. W., 1976. Growth inhibition caused by turbulence in the toxic marine dinoflagellate *Gonyaulax excavata*. *Journal of the Fisheries Research Board of Canada* 33(11):2598-2602.
- Wüest, A. & A. Lorke, 2003. Small-scale hydrodynamics in lakes. *Annual Review of fluid mechanics* 35(1):373-412.
- Xu, D. & J. Chen, 2013. Accurate estimate of turbulent dissipation rate using PIV data. *Experimental Thermal and Fluid Science* 44:662-672.
- Yeung, P. K. K. & J. T. Y. Wong, 2003. Inhibition of cell proliferation by mechanical agitation involves transient cell cycle arrest at G1 phase in dinoflagellates. *Protoplasma* 220(3):173-178.
- Yousif, E. & R. Haddad, 2013. Photodegradation and photostabilization of polymers, especially polystyrene: review. *Springerplus* 2:398-398.
- Zhou, J., X. Han, B. Qin, C. Casenave & G. Yang, 2016. Response of zooplankton community to turbulence in large, shallow Lake Taihu: a mesocosm experiment. *Fundamental and Applied Limnology / Archiv für Hydrobiologie* 187(4):325-324.
- Zirbel, M. J., F. Veron & M. I. Latz, 2000. The reversible effect of flow on the morphology of *Ceratocorys horrida* (Peridinales, Dinophyta). *Journal of Phycology* 36(1):46-58.

APPENDIX 1 - Lesser-used turbulence-generation techniques

Having covered the main techniques used to generate turbulence in the laboratory, it is also worth discussing more novel or lesser-used techniques, including pumping, magnetic stirrers, rotating chambers, wave tanks, impellers/propellers, paddles, dialysis cylinders, and convective mixing.

Pumping: As is common practice in aquaria, water may be introduced via a pump. This manner of turbulence generation is unrepresentative of natural turbulence as mixing would be greatest adjacent to the outflow and would quickly attenuate with distance (Sanford, 1997). Depending on the length of study, the effectiveness of the pumps may become reduced with time due to biofouling clogging pipes and pumps (Kangas and Adey, 2008). Using an array of hydraulic actuator pumps placed at the corners of a cubic tank, Webster et al. (2004) produced near-isotropic homogeneous turbulence comparing the flow characteristics with other studies using grids. The absence of moving structures inside the tank not only facilitates current measurements but also reduced the risk of mechanically damaging the organisms. Subsurface pumps can also be used to simulate surface wind-waves within a tank (Zhou et al., 2016). Laboratory flume tanks also use pump systems to produce specific flow regimes, generating a variety of ϵ under both laminar and turbulent regimes. A number of studies were carried out on different bioluminescent dinoflagellates to ascertain the threshold shear required to make them bioluminesce (Rohr et al., 1990; Latz and Rohr, 1999; Latz et al., 2004; Latz et al., 2009). Once this relationship has been determined, this threshold can be used to calculate the turbulence by recording the bioluminescence intensity. By using aerofoils in a flume tank, Laws et al. (1983) promoted turbulence eddies; as water moves at a critical flow velocity over the aerofoils, pressure differentials above and below produce turbulent vortices resulting in a yield doubling of the diatom *Phaeodactylum tricornutum* Bohlin.

Magnetic stirrers: Magnetic stirring devices are commonly used to agitate chemical solutions. The resulting turbulence profile produced in a vessel is inverted when compared to those in nature.

Typically, a water column will exhibit a wind- and convection-mixed turbulent upper layer with ϵ decreasing with depth. Large flows can cause mixing at depth via bed friction which can result in high levels of turbulence. However, this would need to occur in a water column that is suitably shallow enough to allow this bottom-generated turbulence to propagate up into the photic layer for this to be applicable within a cosm context. In addition, the turbulence field generated from magnetic stirrers is difficult to measure accurately so any biological changes are difficult to attribute to a particular flow characteristic (Warnaars et al., 2006). Researching optimal growth conditions for the dinoflagellate *Cryptocodinium cohnii*, Tuttle and Loeblich (1975) compared cell growth from cultures subjected to rotary shakers and magnetic stirrers before concluding that the shaker intensities used in the experiment damaged cells with no significant increase in growth compared to cultures exposed to magnetic stirring.

Rotating chambers: An enclosed chamber can be constructed that rotates in the z-axis. This technique is useful when studying the effects of vertical mixing especially on species that exhibit gravitaxis or have a preferential swimming / buoyancy direction. Sengupta et al. (2017) made use of a space-saving and cost-effective turbulence generation technique via a millimetre-scale “millifluidic chamber”. Attached to a computer-controlled motor, the chamber could be programmed to mimic vertical overturning, specifically designed to be the same order of magnitude as Kolmogorov scale overturns.

Wave tanks: As with flume tanks, many laboratories now also have separate wave tanks or the ability to convert an existing flume tank. It can be difficult to directly measure the turbulent field associated with wave events due to surface oscillations and cavitation which interfere with velocity probes that need to be constantly submerged. As such, Stokes et al. (2004) developed a novel technique utilising bioluminescent dinoflagellates to correlate the intensity of light emitted to ϵ within a wave. Waves were computer-generated to consistently break at the same location while a

slow-motion digital camera was used to photograph the breaker with pixel light intensity of the image being related to the shear stress the organism was subjected to.

Impellers/propellers: A benefit of using propellers to produce turbulence in the laboratory is that the equipment is relatively low-cost and off-the-shelf, coming in a variety of different sizes and materials. Furthermore, the propellers can be easily attached to variable speed motors to produce a range of turbulent intensities. The propeller / impellor can have a profound effect on the circulation within the tank with radial impellers (vertical blades attached to a horizontal disc) resulting in two pairs of convective cells while axial impellers (akin to a boat propeller) cause a single pair of convective cells. The impellers can be sized appropriately and spin at specific speeds to either promote tank circulation or to generate localised turbulence; Sanford (1997) recommends a balance between these two extremes. A propeller system was used by Garrison and Tang (2014) to test the effect of high intensity episodic turbulence on diatoms noting an increase in cell mortality after exposure of only 45 seconds. Impellor like-structures have been used in a number of longer-duration multi-trophic experiments involving natural populations of phytoplankton and zooplankton (Donaghay and Klos, 1985; Escaravage et al., 1997; Petersen et al., 1998). These set-ups involve a central shaft with rods / paddles attached at specific depths to promote vertical stratification with separate well-mixed layers mirroring an upper wind-mixed layer with a lower mixed layer. The rotational direction is alternated to prevent whirlpool mixing that would transfer water from one layer to another. In order to simulate a reduction in flow that would normally be associated with tidal slack, Petersen et al. (1998) stopped the rotational mixing periodically. Donaghay and Klos (1985) used a variety of horizontal paddles at different depths to produce two separate well-mixed layers; a physical regime found in nature that is difficult to replicate using other methods of turbulence generation.

Paddles: Mechanised paddles can be placed into a cosm with the size, orientation and placement of the paddles altered at the discretion of the researcher. The paddles can oscillate horizontally or

vertically with the agitation produced increasing with distance from the pivot. As such, it may be prudent to opt for a rotating paddle (analogous to a watermill wheel) to ensure more isotropic conditions (Richmond and Vonshak, 1978; Dempsey, 1982).

Dialysis cylinders: Analogous to a small limnocorral, Köhler (1997) placed a natural population of phytoplankton into a 650ml transparent cylinder and suspended it into various aquatic environments. Using a lift system, the cylinder was suspended at depth and oscillated vertically through the water column at various amplitudes, frequencies and durations to mirror natural vertical mixing. The water within the cylinder was homogenised via a single paddle mounted on the inner edge of the cylinder, mixing the internal fluid as the cylinder rolled.

Convective mixing: It is possible to generate convective mixing within a cosm by either applying a heat source at the base (causing the water to rise) or by cooling the surface (causing the water to sink). The convective cell(s) established can be described as a function of water depth and the temperature difference between the top and bottom of the tank; high temperatures on the surface reducing to lower temperatures at depth will clearly result in a classic stratified water column with a distinct thermocline. Inverting this set-up by cooling the surface water and gently heating the water depth will result in a constant thermal instability mimicking the advection of water akin to a turbulent overturn. If carried out in suitably sized cosms (of the scale of natural turbulent overturns), this technique generates vertical turbulent overturns that more closely match those found in nature. Thus, the light climate that the planktonic organisms experience would be more realistic with regards to vertical distances moved. Båmstedt and Larsson (2018) showcased the convective-mixing abilities of the cosm facilities at Umeå Marine Science Centre, Sweden. Each 5m-high mesocosm is surrounded by three vertical sections into which flows a solution which can be heated or cooled to produce specific temperature profiles. This can be used to replicate the natural thermoclinic temperature structures, but by inverting the temperature profile via mild heating at

depth, it is possible to cause convective overturning. A larger temperature difference between the top section and the lower section causes a greater degree of convective flow.

APPENDIX 2 - Lesser-used techniques for quantifying turbulence

Dye dispersion: Dye tracing involves the release of a fluorescent dye product into a mesocosm in order to approximate turbulent mixing. The dye is released at mid-depths and then monitored by either taking water samples at depth, by pumping water at depth through a surface fluorometer or by conducting fluorimetry profiles with depth. Working on the CEPEX array, Steele et al. (1977) used dye dispersion to quantify vertical diffusivity for a number of mesocosm studies (Eppley et al., 1978; Sonntag and Parsons, 1979). By measuring the vertical distribution of the dye with time, Steele et al. (1977) were able to not only observe the gradual homogenisation of the dye concentration but also observed the development of a secondary patch of dye concentration at depth.

Clearly the dye substance that is used to measure flow should be inert so as to not react with any surfaces / materials within the tank. Furthermore, the substance should not be toxic nor should it act as or decay into a chemical species that could influence growth rate of any phytoplankton / bacteria within the experiment. For example, Båmstedt and Larsson (2018) introduced humic acid as a marker dispersant in their initial mixing studies before switching to rhodamine dye. Humic acid can decompose into other bioactive compounds / nutrients so could influence phytoplankton growth with time. Furthermore, the addition of an acid would alter the gas solubility of the water as well as biasing any biological experiment towards low-pH tolerant species. At high concentrations, rhodamine dye would affect light transmission through the water especially towards the UV end of the spectrum.

Bioluminescence: Certain species of dinoflagellates are known to exhibit bioluminescence, producing a brilliant blue light when exposed to species-dependent shear flows. As well as flow regime, dinoflagellate cells have been shown to exhibit bioluminescent tendencies under a variety of rapidly changing factors including thermal, pH, chemical, electrical and osmotic pressure (see

references in Stokes et al. (2004)). While this technique is applicable to flow visualisation in turbulent fields, it is restricted to studies of bioluminescent organisms alone. It is not recommended to add bioluminescent organisms to cosms with other species present as this would bias the population dynamics considerably. Firstly, a number of bioluminescent species are allelopathic, producing toxins that impede motility, growth rates and nutrient uptake rates (Schwartz et al., 2016). Other species, such as *Noctiluca scintillans* (Macartney) Kofoid & Swezy, are carnivorous so would skew population growth measurements via grazing. Furthermore, carnivorous dinoflagellates of this type excrete ammonia which can cause subsequent growth rate changes in different groups (Turkoglu, 2013).

Using colonies of *Pyrocystis fusiformis* C.W.Thomson, Stokes et al. (2004) used a wave tank and an intensified slow-motion camera to record the light emitted by the cells in a breaking wave. Firstly, the cell anxiety parameter for the species is calculated from observations; this factor is an inherent property of the cell which dictates the likelihood that the cell will emit light given a certain environmental perturbation. The pixel intensity is recorded then used to estimate the local shear stress in the fluid medium which can then be converted into shear stress values and ϵ . The digital images produced are effectively 2D maps showing the quantitative evolution of a breaking wave with time.

While this technique can be used to quickly produce a spatial map of ϵ , it does come with some bias namely the presence of bubbles which scatter / absorb the emitted light. It is possible to omit the effects of bubbles by subtracting the mean intensity recorded in a process known as thresholding. Thresholding itself is a subjective process so it is crucial that the same threshold level is applied to all images. The images can be adjusted so as to remove light occurring outside of the perturbation (e.g. behind the breaking wave) and those that exhibit radically different light properties. It is proposed to use a light source of known intensity placed in the sample region so as to properly account for the scattering / absorption effects of bubbles. Another factor to consider is that of cell

memory; a measure of how the cells may adapt to the conditions they are being exposed to and alter their light emission accordingly (Stokes et al., 2004). As well as wave tanks, flume tanks have also been used in studies where the response of a given bioluminescent species can be monitored with regards to different flow rate shear stresses under both laminar and turbulent regimes (Rohr et al., 1990; Latz and Rohr, 1999).

Depending on the level of ε encountered, it is possible to use different bioluminescent species that exhibit different trigger thresholds. In an experiment aiming to observe laminar and turbulent flow in pipes, Latz et al. (2004) experimented with four different dinoflagellate species with the aim of producing a shear sensitivity hierarchy. As well as exhibiting shear thresholds ranging across an order of magnitude, the cells also display a range of morphological differences being fusiform, spherical and spined. As the flow rate in the pipe apparatus was altered in the presence of the different species, light flashes were recorded using a photon-counting photomultiplier system.

APPENDIX 3 - Summary table of known phytoplankton-turbulence experiments

Turbulence Method	Cosm material	Approx. cosm volume (m³)	Organism(s)	Turbulence Dissipation Rate Range (m²/s³) (or equivalent parameter)	Reference
Aeration	Glass	2.5 x 10 ⁻³	Green algae – <i>Dunaliella viridis</i> Teodoresco	6.8 x 10 ⁻⁵ to 4.8 x 10 ⁻³	Aguilera et al. (1994)
Aeration	Glass	1.0 x 10 ⁻³	Green algae – <i>Scenedesmus obliquus</i> (Turpin) Kützing, <i>Stichococcus</i> sp.	None	Bakus (1973)
Aeration	Unspecified	2.5 x 10 ⁻²	Natural population including: Diatoms: <i>Skeletonema costatum</i> (Greville) Cleve, <i>Chaetoceros</i> sp., <i>Lauderia</i> sp., <i>Thalassiosira cf. hyalina</i> (Grunow) Gran, <i>Thalassiosira cf. allenii</i> H.Takano, <i>Pseudonitzschia</i> sp, <i>Guinardia</i> sp.,	10 ⁻³ to 10 ⁻¹	Cózar and Echevarría (2005)

Aeration	Polyethylene	6.65 x 10 ¹	<p>Natural population including:</p> <p>Diatoms – <i>Chaetoceros socialis</i> H.S.Lauder, <i>Stephanopyxis palmeriana</i> (Greville) Grunow, <i>Pseudo-nitzschia pungens</i> (Grunow ex Cleve) Hasle ^a, <i>Coscinodiscus wailesii</i> Gran & Angst</p> <p>Dinoflagellates - <i>Dinophysis</i> sp., <i>Amphidinium</i> sp., <i>Peridinium</i> sp., <i>Gymnodinium</i> sp., <i>Noctiluca</i> sp.</p> <p>Ciliates – <i>Eutintinnus pectinis</i> Kofoid & Campbell, <i>Favella ehrenbergii</i> (Claparède & Lachmann) Jörgensen, <i>Helicostomella subulate</i> (Ehrenberg) Jörgensen, <i>Salpingella curta</i> Kofoid & Campbell</p> <p>Copepods - various</p>	2.15 x 10 ⁻⁹ to 2.51 x 10 ⁻⁸	Eppley et al. (1978)
Aeration	Glass	1.0 x 10 ⁻³	<p>Ciliates – <i>Tetrahymena pyriformis</i> (Ehrenberg), <i>T. thermophila</i>, <i>T. pigmentosa</i></p>	None	Hellung-Larsen and Lyhne (1992)

Aeration	Unknown	Unknown	Diatoms - <i>Chaetoceros curvisetus</i> Cleve, <i>Skeletonema costatum</i>	None	Schöne (1970)
Aeration	Polyethylene	1.67×10^3	Natural population of phytoplankton & zooplankton with salmonids added artificially. Phytoplanktonic species unspecified but main group enumerated.	Vertical eddy diffusivity coefficient = $0.06 \text{cm}^2/\text{s}$ (Steele et al., 1977).	Sonntag and Parsons (1979)
Aeration	Acrylate	3.4×10^{-3}	Diatom – <i>Phaeodactylum tricornutum</i>	None	Thomas et al. (1984a)
Aeration	Acrylate	3.4×10^{-3}	Green algae – <i>Dunaliella primolecta</i> Butcher & <i>Tetraselmis suecica</i> Butcher.	None	Thomas et al. (1984b)
Aeration	Acrylate	3.4×10^{-3}	Golden algae - <i>Isochrysis</i> (Tahitian strain) & <i>Microchloropsis salina</i> (D.J.Hibbard) M.W.Fawley, I.Jameson & K.P.Fawley ^b	None	Thomas et al. (1984c)
Aeration	Glass	4.0×10^{-5}	Dinoflagellate – <i>Cryptocodinium cohnii</i>	None	Tuttle and Loeblich (1975)
Convective heating	Polyethylene	2.03×10^0	None	Dye injection homogenisation timed	Båmstedt and Larsson (2018)

Couette	Unspecified	1.00×10^{-3}	Diatom - <i>Skeletonema</i> sp., <i>Chaetoceros</i> sp.	Converted using Equation (6) 3.42×10^{-5}	Bergkvist et al. (2018)
Couette	Unknown	Unknown	Dinoflagellate - <i>Alexandrium minutum</i> Halim	1.64×10^{-2} (Berdalet et al., 2007)	Chen et al. (1998)
Couette	Acrylate / steel	4.16×10^{-4}	Green algae - <i>Chlorella</i> sp.	Converted using Equation (6) 1.28×10^{-2}	Davis et al. (1953)
Couette	Glass	8.78×10^{-4}	Dinoflagellate – <i>Lingulodinium polyedra</i> ^c	Converted using Equation (6) 7.96×10^{-9} to 1.82×10^{-3}	Gibson and Thomas (1995)
Couette	Unspecified	8.79×10^{-4}	Green algae – <i>Desmodesmus communis</i> (E.Hegewald) E.Hegewald ^k	1.27×10^{-3} to 3.13×10^{-1}	Hondzo et al. (1997)
Couette	Glass	1.56×10^{-4}	Dinoflagellate – <i>Lingulodinium polyedra</i> ^c	1.00×10^{-5} to 3.50×10^{-4}	Juhl and Latz (2002)
Couette	Glass	1.56×10^{-4}	Dinoflagellate – <i>Lingulodinium polyedra</i> ^c	Converted using Equation (6) 1.88×10^{-5}	Juhl et al. (2000)
Couette	Acrylate	3.91×10^{-4}	Dinoflagellate – <i>Alexandrium catenella</i> (Whedon & Kofoid) Balech ^d	1.0×10^{-5}	Juhl et al. (2001)

Couette	Acrylate	8.0×10^{-4}	Diatoms - <i>Skeletonema costatum</i> , <i>Thalassiosira nordenskioldii</i> P.T. Cleve	2.5×10^{-7}	Karp-Boss and Jumars (1998)
Couette	Acrylate	8.0×10^{-4}	Dinoflagellates - <i>Glenodinium foliaceum</i> F.Stein, <i>Alexandrium catenella</i> ^d	1.0×10^{-8} to 1.0×10^{-5}	Karp-Boss et al. (2000)
Couette	Acrylate	2.38×10^{-4}	Dinoflagellates – <i>Lingulodinium polyedra</i> ^c , <i>Pyrocystis noctiluca</i> Murray ex Haeckel, <i>P. fusiformis</i>	Converted using Equation (6) Large tanks = 9.65×10^{-4} to 6.86×10^{-1} Small tanks = 3.86×10^{-3} to 2.75×10^0	Latz et al. (1994)
Couette	Unspecified	1.23×10^{-3}	Cyanobacteria – <i>Nodularia sphaerocarpa</i> Bornet & Flahault, <i>N. spumigena</i> Mertens ex Bornet & Flahault	4.66×10^{-6} to 3.23×10^{-4}	Moisander et al. (2002)
Couette	Acrylate	6.45×10^{-4}	Diatom – <i>Ditylum brightwellii</i> (T.West) Grunow	5.94×10^{-11} to 5.0×10^{-8}	Pasciak and Gavis (1975)
Couette	Polycarbonate	1.51×10^{-4}	Dinoflagellate – <i>Pfiesteria piscicida</i> Steidinger & J.M.Burkholder with cryptophyte food source <i>Storeatula major</i> D.R.A.Hill	2.38×10^{-10} to 2.88×10^{-8}	Stoecker et al. (2006)

Couette	Glass	6.45×10^{-4}	Dinoflagellate – <i>Lingulodinium polyedra</i> ^c	4.50×10^{-6} to 1.64×10^{-2}	Thomas and Gibson (1990a)
Couette	Glass	6.45×10^{-4}	Dinoflagellate – <i>Lingulodinium polyedra</i> ^c	1.80×10^{-5} to 1.64×10^{-2}	Thomas and Gibson (1990b)
Couette	Glass	Unspecified	Dinoflagellate – <i>Akashiwo sanguinea</i> ^e	2.8×10^{-7} to 1.8×10^{-3}	Thomas and Gibson (1992)
Couette	Unknown	Unknown	Dinoflagellates – <i>Akashiwo sanguinea</i> ^e , <i>Prorocentrum micans</i> Ehrenberg	4.6×10^{-4} (Berdalet et al., 2007)	Tynan (1993)
Dialysis chamber	Glass	6.5×10^{-4}	Natural population including: Diatom – <i>Scenedesmus</i> sp., <i>Cymbella</i> sp. <i>Navicula</i> sp., <i>Diatoma</i> sp. Green Algae – <i>Chlamydomonas</i> sp. Cryptophyte – <i>Cryptomonas</i> sp.	None	Köhler (1997)

Grid - horizontal	Glass	4.9×10^{-3}	Green Algae – <i>Nephroselmis olivacea</i> F.Stein, <i>Cryptomonas curvata</i> Ehrenberg, <i>Spondylosium pulchellum</i> (W.Archer) W.Archer, <i>Pediastrum boryanum</i> (Turpin) Meneghini Diatoms – <i>Asterionella formosa</i> Hassall, <i>Aulacoseira granulata</i> (Ehrenberg) Simonsen	7.9×10^{-5} to 7.8×10^{-3}	Fraisse et al. (2015)
Grid - horizontal	Acrylate	9.28×10^{-4}	Dinoflagellate – <i>Heterosigma akashiwo</i> (Y.Hada) Y.Hada ex Y.Hara & M.Chihara	2.0×10^{-9} to 1.6×10^{-8}	Linares (2015)
Grid - horizontal	Unspecified	6.65×10^{-3}	Dinoflagellate – <i>Phaeocystis globosa</i>	1.0×10^{-6} to 1.0×10^{-4}	Schapira et al. (2006)
Grid - horizontal	Acrylate	3.05×10^{-2}	Green algae – <i>Selenastrum capricornutum</i>	9.60×10^{-9} to 1.25×10^{-6}	Warnaars et al. (2006)
Grid - vertical	Acrylate	3.0×10^{-2}	Natural population with a focus on phytoplankton biomass and copepod <i>Acartia italica</i> Steuer	Vertical eddy diffusivity = $0.5 \text{ cm}^2/\text{s}$ (unstirred) / $1 \text{ to } 5 \text{ cm}^2/\text{s}$ (stirred).	Alcaraz et al. (1988)
Grid - vertical	Acrylate	2.92×10^{-1}	Marine snow – Diatom aggregates of <i>Chaetoceros</i> sp. and <i>Nitzschia</i> sp.	1.0×10^{-7} to 1.0×10^{-4}	Allredge et al. (1990)

Grid - vertical	Acrylate	1.5×10^{-2}	Natural population (filtered through a 150 μm mesh) including: Bacteria – <i>Synechococcus</i> sp., <i>Prochlorococcus</i> sp.	5.5×10^{-6}	Arin et al. (2002);
Grid - vertical	Acrylate	1.5×10^{-2}	Natural population (filtered through a 150 μm mesh) including: Diatoms – <i>Chaetoceros</i> sp, <i>Pseudo-nitzschia</i> sp	5.5×10^{-6}	Maar et al. (2002)
Grid - vertical	Acrylate	2.60×10^0	Natural population (filtered through 250 μm filter) including: Diatoms - <i>Chaetoceros</i> sp., <i>Cylindrotheca closterium</i> (Ehrenberg) Reimann & J.C.Lewin, <i>Dactyliosolen fragilissimus</i> (Bergon) Hasle, <i>Nitzschia longissima</i> (Brébisson) Ralfs, <i>Skeletonema costatum</i> , <i>Thalassiosira</i> sp.	2.0×10^{-9} to 1.0×10^{-4}	Beauvais et al. (2006)
Grid - vertical	Glass	1.0×10^{-3}	Dinoflagellates – <i>Akashiwo sanguinea</i> ^e	2.0×10^{-3}	Berdalet (1992)
Grid - vertical	Glass	4.0×10^{-3}	Dinoflagellates - <i>Alexandrium minutum</i> , <i>Akashiwo sanguinea</i> ^e	1×10^{-4}	Berdalet and Estrada (1993)

Grid- vertical	Acrylate	1.38×10^{-2}	Bacteria – <i>Vibrio splendidus</i> Flagellate – <i>Paraphysomonas</i> sp.	1.00×10^{-5} to 1.35×10^{-5}	Delaney (2003)
Grid - vertical	Acrylate	2.0×10^{-3}	Ciliate – <i>Strombidium sulcatum</i> Claparède & Lachmann	5.0×10^{-7} to 2.0×10^{-4}	Dolan et al. (2003)
Grid - vertical	Acrylate	3.0×10^{-2}	Natural population including: Diatoms – <i>Chaetoceros</i> sp., <i>Thalassiosira</i> sp., <i>Leptocylindrus danicus</i> Cleve, <i>Skeletonema</i> <i>costatum</i> , <i>Cylindrotheca closterium</i> Dinoflagellates – <i>Protoperidinium</i> sp, <i>Scrippsiella trochoidea</i> (F.Stein) A.R.Loeblich III Haptophyte – <i>Emiliana huxleyi</i> (Lohmann) W.W.Hay & H.P.Mohler	Vertical eddy diffusivity = 0.5 cm^2/s (unstirred) / 1 to 5 cm^2/s (stirred).	Estrada et al. (1987)

Grid - vertical	Polyethylene	2.50×10^0	Natural population filtered through 250µm filter including: <i>Chaetoceros</i> sp., <i>Cylindrotheca closterium</i> , <i>Dactyliosolen fragilissimus</i> , <i>Nitzschia longissima</i> , <i>Skeletonema costatum</i> , <i>Thalassiosira</i> sp. (Beauvais et al., 2006)	1.0×10^{-7} to 1.0×10^{-6}	(Guadayol et al., 2009a)
Grid - vertical	Acrylate	2.0×10^{-3}	Dinoflagellate – <i>Oxyrrhis marina</i> Dujardin Haptophyte – <i>Isochrysis</i> sp.	1.0×10^{-8} to 1.0×10^{-4}	Havskum (2003)
Grid - vertical	Acrylate	2.0×10^{-3}	Dinoflagellate – <i>Kryptoperidinium triquetrum</i> (Ehrenberg) U.Tillmann, M. Gottschling, M.Elbrächter, W.-H.Kusber & M.Hoppenrath ^f	1.0×10^{-8} to 1.0×10^{-4}	Havskum and Hansen (2006)
Grid - vertical	Acrylate	2.0×10^{-3}	Dinoflagellates – <i>Fragilidium subglobosum</i> & <i>Tripos muelleri</i> Bory ^g	1.0×10^{-8} to 1.0×10^{-4}	Havskum et al. (2005)
Grid - vertical	Fibreglass	3.02E+00	Natural population (phytoplankton dominated by <i>Anabaena</i> sp.)	2.0×10^{-4} to 3.80×10^{-3}	Howarth et al. (1993)
Grid - vertical	Acrylate	2.60×10^0	see Beauvais et al. (2006)	2.0×10^{-9} to 1.0×10^{-4}	Iversen et al. (2009)

Grid - vertical	Unspecified	Unspecified	Dinoflagellates – <i>Peridiniella danica</i> (Paulsen) Y.B.Okolodkov & J.D.Dodge, <i>Gyrodinium dominans</i> Hulbert, <i>Oxyrrhis marina</i> Ciliate – <i>Mesodinium pulex</i> Claparède & Lachmann	1.2 x 10 ⁻⁶	Martínez et al. (2017)
Grid - vertical	Unspecified	2.40 x 10 ⁰	Natural population filtered through 250µm filter – no specific species reported.	1.0 x 10 ⁻⁷ to 1.0 x 10 ⁻⁴	Metcalfe et al. (2004)
Grid - vertical	Polyethylene	2.70 x 10 ¹	Natural plankton population including: Flagellate – <i>Ebria tripartita</i> (Schumann) Lemmermann Diatom – <i>Skeletonema costatum</i> Ciliate – <i>Mesodinium rubrum</i> (Lohmann) Leegard, <i>Cyclotrichium</i> sp. Copepods – <i>Calanus helgolandicus</i> Claus, <i>Calanus finmarchicus</i> Gunnerus	5.3 x 10 ⁻⁹ to 1.7 x 10 ⁻⁷ (Svensen et al., 2001)	Nejstgaard et al. (2001a)

Grid - vertical	Polyethylene	2.70 x 10 ¹	<p>Natural plankton population including:</p> <p>Flagellate – <i>Octactis speculum</i> (Ehrenberg)</p> <p>F.H.Chang, J.M.Grieve & J.E.Sutherland ¹,</p> <p><i>Emiliana huxleyi</i>, <i>Ebria tripartita</i></p> <p>Diatom – <i>Skeletonema costatum</i>, <i>Amphiprora sp</i></p> <p>Ciliates – <i>Strombidium spp.</i> and <i>Strombilidium spp.</i></p> <p>Copepods – <i>Calanus helgolandicus</i></p>	<p>5.3 x 10⁻⁹ to 1.7 x 10⁻⁷</p> <p>(Nerheim et al., 2002)</p>	<p>Nejstgaard et al. (2001b)</p>
-----------------	--------------	------------------------	---	---	----------------------------------

Grid - vertical	Unspecified	1.30×10^1	<p>Natural population including:</p> <p>Dinoflagellates – <i>Peridinium</i> sp.</p> <p>Diatoms – <i>Skeletonema costatum</i>, <i>Chaetoceros compressus</i> Lauder, <i>Chaetoceros affinis</i> Lauder, <i>Chaetoceros didymus</i> Ehrenberg, <i>Chaetoceros perpusillus</i> Cleve, <i>Cylindrotheca fusiformis</i> Reimann & J.C.Lewin, <i>Leptocylindricus danicus</i> Cleve, <i>Rhizosolenia delicatula</i> Cleve</p> <p>Golden Algae – <i>Dinobyron</i> sp.</p> <p>Copepods - various</p>	None	Oviatt (1981)
Grid - vertical	Glass	1.0×10^{-4}	<p>Flagellate – <i>Paraphysomonas imperforata</i></p> <p>I.A.N.Lucas</p>	8.5×10^{-5} to 8.6×10^{-1}	Peters and Gross (1994)
Grid - vertical	Glass	1.0×10^{-4}	<p>Flagellate – <i>Paraphysomonas imperforata</i></p>	5.0×10^{-6} to 1.5×10^{-3}	Peters et al. (1996)
Grid - vertical	Acrylate	1.5×10^{-2}	<p>Natural population – no species identified but groups of bacteria, flagellates and ciliates.</p>	5.3×10^{-6} to 5.9×10^{-6}	Peters et al. (2002)

Grid - vertical	Acrylate	1.7×10^{-2}	Cyanobacteria – <i>Microcystis aeruginosa</i> (Kützing) Kützing	Turbulent intensity ranged from 7.1×10^{-3} and 7.04×10^{-2} m/s	Regel et al. (2004)
Grid - vertical	Glass	2.5×10^{-2}	Diatom – <i>Phaeodactylum tricornutum</i> . Dinoflagellate – <i>Brachionomonas submarina</i> Bohlin	2.3×10^{-4} to 2.3×10^{-1}	Savidge (1981)
Grid - vertical	Polycarbonate	1.2×10^{-2}	Dinoflagellates – <i>Alexandrium catenella</i> ^d , <i>A. tamarense</i> ^h , <i>Tripos fusus</i> (Ehrenberg) F.Gómez ^j , <i>Tripos muelleri</i> ^g , <i>Gymnodinium catenatum</i> H.W.Graham, <i>Gyrodinium sp.</i> , <i>Lingulodinium polyedra</i> ^c , <i>Pyrocystis fusiformis</i> , <i>P. noctiluca</i>	1.0×10^{-8} to 1.0×10^{-4}	Sullivan and Swift (2003)

Grid - vertical	Polyethylene	2.70 x 10 ¹	Diatoms – <i>Chaetoceros socialis</i> Flagellates – <i>Resultor micron</i> (Thronsen) Moestrup, <i>Nephroselmis minuta</i> (N.Carter) Butcher Haptophytes – <i>Phaeocystis pouchetii</i> (Hariot) Lagerheim Dinoflagellates - unspecified	5.3 x 10 ⁻⁹ to 1.9 x 10 ⁻⁷	Svensen et al. (2001)
Inversion	Acrylate	7.68 x 10 ⁻⁸	Raphidophyte – <i>Heterosigma akashiwo</i> (primarily)	3.0 x 10 ⁻⁸	Sengupta et al. (2017)
Magnetic	Glass	1.0 x 10 ⁻⁴	Dinoflagellates – <i>Scrippsiella lachrymosa</i> J.Lewis ex Head	None	Smith and Persson (2005)
Magnetic	Glass	4.0 x 10 ⁻⁵	Dinoflagellate – <i>Cryptocodinium cohnii</i>	None	Tuttle and Loeblich (1975)
Paddles	Unspecified	Unspecified	Dinoflagellate – <i>Kryptoperidinium triquetrum</i> ^f , <i>Alexandrium tamarense</i> ^h Diatom – <i>Skeletonema costatum</i>	1.0 x 10 ⁻⁵	Dempsey (1982)

Paddles	PVC	1.30 x 10 ¹	Natural population including: Diatom – <i>Skeletonema costatum</i> Zooplankton – various copepods	None	Donaghay and Kloss (1985)
Paddles	Glass	3.78 x 10 ⁻²	Diatom – <i>Thalassiosira weissflogii</i> (Grunow) G.A.Fryxell and Hasle, <i>Skeletonema costatum</i> Cryptomonad – <i>Rhodomonas salina</i> (Wislouch) D.R.A.Hill & R.Wetherbee Chlorophyte – <i>Dunaliella tertiolecta</i> Butcher	1.1 x 10 ⁻⁴ to 4.0 x 10 ⁻⁴	Garrison and Tang (2014)
Paddles	Acrylate	1.3 x 10 ⁻¹	Natural population including: Cyanobacteria - <i>Oscillatoria</i> spp, <i>Prochlorothrix hollandica</i> Burger-Wiersma, Stal & Mur	None	Kromkamp et al. (1992)
Paddles	Fibreglass	1.00E+00	Natural population – no species identified but chlorophyll-a and other pigments used to quantify populations of diatoms, cyanobacteria and cryptophytes.	3.00 x 10 ⁻⁷ to 6.89 x 10 ⁻⁵	Petersen et al. (1998)
Paddles	Natural	Unspecified	Cyanobacteria – <i>Arthrospira</i> sp. (aka <i>Spirulina</i>)	None	Richmond and Vonshak (1978)

Paddles	Acrylate	1.3×10^{-1}	Cyanobacteria – <i>Prochlorothrix hollandica</i>	None	Rijkeboer et al. (1990)
Paddles	Unknown	Unknown	Diatoms - <i>Asterionellopsis glacialis</i> (Castracane) Round, <i>Skeletonema costatum</i>	Unknown	Thomas et al. (1997)
Pumping	Acrylate	7.5×10^{-2}	Dinoflagellates - <i>Lingulodinium polyedra</i> ^c	Shear stress ranged from 0.2 N/m ² to 10 N/m ²	Latz and Rohr (1999)
Pumping	Acrylate	7.5×10^{-2}	Dinoflagellates – <i>Tripos fusus</i> ^j , <i>Ceratocorys horrida</i> , <i>Lingulodinium polyedra</i> ^c , <i>Pyrocystis fusiformis</i>	Shear stress ranged from 0.2 N/m ² to 10 N/m ²	Latz et al. (2004)
Pumping	Fibreglass	4.15×10^0	Diatom – <i>Phaeodactylum tricornutum</i>	Shear stress ranged from 0.02 N/m ² to 0.3 N/m ²	Laws et al. (1983)
Pumping	Acrylate	5.0×10^{-2}	Natural plankton population including: Cyanobacteria - <i>Limnothrix</i> sp., <i>Aphanizomenon</i> sp. Yellow-green algae - <i>Tribonema</i> sp. Green algae - <i>Closterium</i> sp., <i>Monoraphidium</i> sp.	Flow of 2.5 mL/s resulting in a mean upward velocity of $7.6 \pm$ 1.4 mm/s.	Pannard et al. (2007)

Pumping	Steel	7.5×10^{-2}	Dinoflagellates – <i>Lingulodinium polyedra</i> ^c , <i>Tripos fusus</i> ^j , and <i>Protoberidinium</i> sp.	5.3×10^{-9} to 1.7×10^{-7}	Rohr et al. (1990)
Pumping	Steel	7.5×10^{-2}	Dinoflagellates – <i>Lingulodinium polyedra</i> ^c , <i>Tripos fusus</i> ^j , and <i>Protoberidinium</i> sp.	5.3×10^{-9} to 1.7×10^{-7}	Rohr et al. (1997)
Pumping	Steel	4.5×10^{-1}	Dinoflagellates – <i>Lingulodinium polyedra</i> ^c , <i>Tripos fusus</i> ^j , and <i>Protoberidinium</i> sp.	Mean shear stress = 11 to 13.5 dyn/cm ²	Rohr et al. (2002)
Shaker - unspecified	Glass	2.5×10^{-3}	Diatom – <i>Chaetoceras affinis</i>	None	Talling (1960)
Shaker - orbital	Glass	3.0×10^{-3}	Dinoflagellates – <i>Akashiwo sanguinea</i> ^e	2.0×10^{-3}	Berdalet (1992)
Shaker - orbital	Glass	4.0×10^{-3}	Dinoflagellates - <i>Scrippsiella trochoidea</i> , <i>Prorocentrum micans</i>	2.0×10^{-4}	Berdalet and Estrada (1993)
Shaker - orbital	Glass	3.0×10^{-3}	Dinoflagellates – <i>Gymnodinium</i> sp., <i>Alexandrium minutum</i> , <i>Prorocentrum triestinum</i> J.Schiller	2.7×10^{-5} to 2.4×10^{-3}	Berdalet et al. (2007)
Shaker - orbital	Glass	1.0×10^{-4}	Cyanobacteria – <i>Anabaena cylindrica</i>	None	Fogg and Than- Tun (1960)

Shaker - orbital	Glass / polycarbonate	3.00×10^{-3}	None	1×10^{-10} to 1×10^{-2}	Guadayol et al. (2009b)
Shaker - orbital	Glass	2.5×10^{-5}	Ciliates – <i>Tetrahymena pyriformis</i> , <i>T. thermophile</i> , <i>T. pigmentosa</i>	1.17×10^{-2} to 2.16×10^{-2}	Hellung-Larsen and Lyhne (1992)
Shaker - orbital	Glass	3×10^{-3}	Dinoflagellates - <i>Prorocentrum micans</i> , <i>Scrippsiella trochoidea</i> , <i>Alexandrium minutum</i>	2.7×10^{-3}	Llaveria et al. (2010)
Shaker - orbital	Glass	1.0×10^{-4}	Diatom – <i>Ditylum brightwellii</i>	None	Pasciak and Gavis (1975)
Shaker - orbital	Polycarbonate	2.5×10^{-3}	Diatoms – <i>Thalassiosira pseudonana</i> Hasle & Heimdal, <i>Coscinodiscus</i> sp	1.0×10^{-3}	Peters et al. (2006)
Shaker - orbital	Unspecified	Unspecified	Dinoflagellates – <i>Peridinium cinctum</i> (O.F.Müller) Ehrenberg	4.3×10^{-3}	Pollinger and Zemel (1981)
Shaker - orbital	Glass	2.5×10^{-4}	Dinoflagellate – <i>Lingulodinium polyedra</i> ^c	2.0×10^{-2}	Thomas and Gibson (1990b)
Shaker - orbital	Glass	4.0×10^{-5}	Dinoflagellate – <i>Cryptocodinium cohnii</i>	None	Tuttle and Loeblich (1975)

Shaker - orbital	Glass	5.0×10^{-5}	Dinoflagellates – <i>Alexandrium tamarense</i> ^h	4.30×10^{-3} to 1.19×10^{-2}	White (1976)
Shaker - orbital	Glass	6.0×10^{-5}	Dinoflagellates – <i>Cryptocodinium cohnii</i> ; <i>Kryptoperidinium triquetrum</i> ^f	1.0×10^{-5} to 9.9×10^{-5}	Yeung and Wong (2003)
Shaker - orbital	Glass	6.0×10^{-5}	Dinoflagellates – <i>Cryptocodinium cohnii</i> ; <i>Kryptoperidinium triquetrum</i> ^f	1.0×10^{-5} to 9.9×10^{-5}	Yeung et al. (2006)
Shaker - orbital	Glass	1.25×10^{-4}	Dinoflagellates - <i>Ceratocorys horrida</i>	1×10^{-5} to 1×10^{-4} (Berdalet et al., 2007)	Zirbel et al. (2000)
Shaker - reciprocal	Glass	2.5×10^{-5}	Ciliates – <i>Tetrahymena pyriformis</i> , <i>T. thermophile</i> , <i>T. pigmentosa</i>	1.17×10^{-2} to 2.16×10^{-2}	Hellung-Larsen and Lyhne (1992)
Shaker - reciprocal	Glass	2.6×10^{-4}	Dinoflagellate - <i>Lingulodinium polyedra</i> ^c	Estimated using Equation (2) ~10	Juhl and Latz (2002)
Wave	Unspecified	9.90×10^0	Dinoflagellate – <i>Pyrocystis fusiformis</i>	3.0×10^{-2} to 3.0×10^1	Stokes et al. (2004)

- ^a The diatom *Pseudo-nitzschia pungens* (Grunow ex Cleve) Hasle 1993 was formerly referred to as *Nitzschia pungens* Grunow ex Cleve 1897.
- ^b The golden alga *Microchloropsis salina* (D.J.Hibbard) M.W.Fawley, I.Jameson & K.P.Fawley 2015 was formerly referred to as *Monallantus salina* Bourrelly 1958.
- ^c The dinoflagellate *Lingulodinium polyedra* (F.Stein) J.D.Dodge 2018 was formerly referred to as *L. polyedrum* Dodge 1989 & *Gonyaulax polyedra* Stein 1883.
- ^d The dinoflagellate *Alexandrium catenella* (Whedon & Kofoid) Balech, 1985 was formerly referred to as *Alexandrium fundyense* Balech, 1985
- ^e The dinoflagellate *Akashiwo sanguinea* (K. Hirasaka) Gert Hansen & Moestrup 2000 was formerly referred to as *Gymnodinium nelsonii* Martin 1929, *G. sanguineum* Hirasaka 1922 & *G. splendens* Lebour 1925.
- ^f The dinoflagellate *Kryptoperidinium triquetrum* (Ehrenberg) U.Tillmann, M. Gottschling, M.Elbrächter, W.-H.Kusber & M.Hoppenrath 2019 was formerly referred to as *Heterocapsa triquetra* (Ehrenberg) F.Stein 1883.
- ^g The dinoflagellate *Tripos muelleri* Bory 1826 was formerly referred to as *Ceratium tripos* (O.F.Müller) Nitzsch 1817.
- ^h The dinoflagellate *Alexandrium tamarense* (Lebour) Balech 1995 was formerly referred to as *A. tamarensis* Balech 1992, *Gonyaulax excavata* Balech 1971 & *G. tamarensis* Lebour 1925.
- ⁱ The flagellate *Octactis speculum* (Ehrenberg) F.H.Chang, J.M.Grieve & J.E.Sutherland 2017 was formerly referred to as *Dictyocha speculum* Ehrenberg 1839.
- ^j The dinoflagellate *Tripos fusus* (Ehrenberg) F.Gómez 2013 was formerly referred to as *Ceratium fusus* (Ehrenberg) Dujardin 1841.
- ^k The green alga *Desmodesmus communis* (E.Hegewald) E.Hegewald 2000 was formerly referred to as *Scenedesmus quadricauda* Chodat 1926

The presence of an 'unknown' indicates a paper that was not available; 'unspecified' indicates that this information was absent from the paper.